Theor Chem Acc (2005) 114: 357–379
DOI 10.1007/s00214-005-0686-4

REGULAR ARTICLE

Franziska Schulz · Bernd Hartke

A new proposal for the reason of magic numbers in alkali cation microhydration clusters

Received: 13 June 2005 / Accepted: 13 July 2005 / Published online: 20 September 2005

Abstract Alkali cation microhydration clusters $M^+(H_2O)_n$, $n \leq 24$, M = Na, K, Cs, have been globally optimised, using a specialised version of genetic algorithms and the common TIP4P/OPLS model potential. The results constitute a first unbiased and systematic overview on structures of alkali cation microhydration clusters. Simple reasons for differing structural trends could be provided. Dodecahedral cages occur, but do not play as prominent a role as frequently believed. In particular, they do not seem to determine the occurrence of magic numbers. A structural pattern all magic number cluster structures do have in common is that only three and/or four-coordinated water molecules can be observed. Molecular dynamics simulations were run in the canonical ensemble, and free energy differences of dissociating clusters were obtained, with dodecahedral cages again showing no special feature. Structures containing only three and/or four-coordinated water molecules, however, are more stable than others thus arriving at a possible explanation for magic numbers.

Keywords Global optimisation · Solvation · Clathrates · Hydrogen bonds · Constrained molecular dynamics · Free energy

1 Introduction

Water may doubtlessly be regarded as the most important solvent on earth. Despite the abundance of literature on this topic even systems like simple ions, for instance alkali cations, solvated by water are still difficult to simulate theoretically and hence are still not completely understood. A simplified approach is the microsolvation clusters $M^+(H_2O)_n$ (with M = Li, Na, K, Rb, Cs and $n = 1, 2, \ldots$) in the gas phase [1,2], since their reduced and controlled size promises an easier treatment. Indeed, it was found that small "nanodroplets" of water molecules can also provide a suitable medium for the investigation of a wide variety of aqueous reactions (see ref. [3] and references therein). Also these systems are accessible both experimentally (see the review articles [3–6] and refs. [7,8]) and theoretically (on moderate ab-initio levels [9,10] and with empirical potentials [11–15], see also further literature cited in these articles).

From the beginning of these experimental investigations, it was found that clusters with certain values of n are "magic numbers" (in particular $n = 20$, but to a lesser degree also various smaller and larger values), i.e. they occur with increased abundance, compared to their immediate neighbours $n - 1$ and $n + 1$. The existence of magic numbers in these systems is usually explained with the possible formation of cage inclusion compounds, in particular that of a dodecahedron of water molecules around the cation in the centre at $n = 20$. This so-called dodecahedron hypothesis is often ascribed to Holland and Castleman [16] but definitely has a longer history (see citations in Kassner and Hagen [17]). This type of cage structures, predominantly those with hydrophobic guest molecules, is well known in the extended solid state as clathrate hydrates. They can be found in a vast number of natural and technological processes [18,19] and hence are examined both experimentally (see, e.g. ref. [20] and references therein) and theoretically (see, e.g. [21] and references therein). Therefore, this explanation had a natural appeal and in consequence served as ad hoc hypothesis in many contexts, from ab initio calculations [22] and rationalisation of microsolvation experiments [7,23,24] up to attempts to understand solvation of hydrophobic groups in the gas phase [8] and in liquid [25,26].

Nevertheless this explanation retained its hypothetical status as it suffered from some shortcomings [27]. In particular, it cannot explain the common observation [7] that $n = 20$ is a magic number for M = K, Rb, Cs, but not for M = Na. In fact, this is no artefact of limited-size microsolvation clusters as bulk solvation simulations indicated characteristical differences between Na^+ and K^+ (see ref. [28] and

F. Schulz · B. Hartke (✉)
Institut für Physikalische Chemie,
Christian-Albrechts-Universität zu Kiel
Olshausenstrasse 40, 24098 Kiel, Germany
Fax: +49-431-8801758
E-mail: hartke@phc.uni-kiel.de

references therein). In addition to the attachment of labels like "structure-making" or "structure-breaking" no detailed explanations for these differences appear to be available, even though biological systems like ion channels in cell membranes may rely on them.

Methods which can be used for global geometry optimisation of cluster structures are in general fairly expensive [29,30]. Genetic algorithm [31–36,38] are a relatively new method for global geometry optimisation of cluster structures. Compared to the other global optimisation methods, genetic algorithms are very reliable in finding the global minimum while being fairly cheap.

Another advantage of some global geometry optimisation methods is that in practice they yield not only the global minimum energy structures, but also an extensive list of low-energy minimum structures. Nevertheless, they only yield a static picture at 0K. Hence it is often argued that in principle global geometry optimisation of a system is irrelevant, as it is not directly comparable to experiment, because (1) experiments are performed above 0K where a Boltzmann distribution of isomers exists and (2) no information on entropy and kinetic effects can be obtained by a plain geometry optimisation. Therefore a better approach would be a full, statistically complete, molecular dynamics or Monte Carlo simulation. Whereas it is possible to gain pieces of information from single molecular dynamics or Monte Carlo trajectories, a study of statistically correct molecular dynamics or Monte Carlo simulation of clusters of this size is still very expensive. One solution would be to combine global geometry optimisation with molecular dynamics simulation and hence gain information on the important regions in configuration space which are likely to be most relevant for a dynamical simulation. In this way it is possible to get a relatively complete overview on the dynamics of these systems on a reasonable time-scale. This approach was chosen in this study.

The aim of this work was to gain structural information about alkali cation microhydration clusters, i.e. $Na^+(H_2O)_n$, $K^+(H_2O)_n$ and $Cs^+(H_2O)_n$ with $4 \leq n \leq 24$, both in general and with a special focus on magic numbers and cage inclusion structures. First a brief overview on the methods used will be given. We will then present the obtained results. The latter section is split according to the results obtained from global geometry optimisation and molecular dynamics simulation. In a final concluding chapter we will give an overview of how these two methods work together and whether or not additional conclusions can be drawn using this combination.

2 Computational methods

An eligible level for the computation of these systems would of course be direct ab initio simulation of bulk solvation, including an extensive treatment of electron correlation and a quantum mechanical treatment of at least the nuclear degrees of freedom involved in hydrogen bonds. However, this is impossible to realise, even in the near future. Consequently both an MD-style approach and a reliable global geometry optimisation at a really appropriate level of electronic structure theory still range at the border to the impossible. Hence the problem had to be tackled from the other end: we applied geometry optimisation to our systems of interest using a common model potential, subsequently utilising the structural information for ensuing molecular dynamics simulations. We emphasise that this is a first step only, nevertheless reliable and convenient: on this level of theory, the global minimum structures can be found with sufficient reliability in practice. Furthermore, the simple nature of the model potential and its restriction to a few separate interaction terms allow for a direct connection of features of the model potential to the cluster structures found, thus arriving at simple explanations for structural trends and also for the dynamics of the structures which allows to build an interesting basis for comparison for future studies on better model potentials and on the ab initio level.

2.1 Model potential

For water–water and water–ion interactions, the well-known TIP4P/OPLS model is used [39,40]. In this model, the water monomers are rigid, while interactions between two monomers m and n are described by a pair potential, see Equ. 1, consisting of a Lennard-Jones term between the locations of the oxygen atoms and of Coulomb terms between partial charges on the hydrogen atoms and on a dummy site Z on the HOH-angle bisector, somewhat off the oxygen atom:

$$v_{mn} = \sum_{i \in m} \sum_{j \in n} \frac{q_i q_j}{r_{ij}} + \frac{A_{mn}}{r_{OO}^{12}} - \frac{C_{mn}}{r_{OO}^{6}}. \quad (1)$$

Water–cation interactions are modelled similarly, with the ion being treated like a water oxygen atom, except that it has a full charge of $+1.0$ assigned to its location. The parameters for Na^+, K^+ and Cs^+ are taken from the literature [41,42] and calculated according to ref. [27]. For the justification of using this particular model potential for the global geometry optimisation see also ref. [27].

2.2 Cluster structure: global geometry optimisation

Global cluster geometry optimisation employing genetic algorithms (GA) has been pioneered in our lab [31] and developed into a reliable and efficient tool for atomic [33] and molecular [34] clusters (see also the overviews in refs. [43,44]). Applications have ranged from pure atomic rare gas clusters [32,33] to mixed molecular clusters [36] using empirical potentials [38] and DFT calculations [45] all the way to full ab initio studies [35].

The version used in the present work and in our earlier investigation of the related $Na^+(H_2O)_n$ system [36] is largely identical to the algorithm described in detail in our benchmark application to pure water clusters [34]. A few minor

technical items have been modified, as described in ref. [36]. The parameters used (population sizes, mutation rates, etc.) are also identical to those described and tested in ref. [34]. As demonstrated there, this enables us to reach reasonable levels of confidence in having actually located the global minima, up to cluster sizes of approximately $n = 22$–25, within a few days of CPU time per run on a single Pentium III processor.

2.3 Cluster dynamics: molecular dynamics simulation

As already explained above, we combined global geometry optimisation with molecular dynamics simulation. We simply used the various global minima as well as some selected local minimum energy structures obtained by the global optimisation as input geometries for the molecular dynamics simulations. This provides a method of investigating the dynamics on the potential energy surface in the region of the global and low-lying local minimum energy structures with rather short and simple MD runs, without the need for unrealistically high temperatures or advanced sampling techniques to overcome high barriers between various regions of configuration space, since we can rely on the global optimisation to have done this work already.

For the purpose of this study, we have written a rigid-body MD routine of our own which contains exactly the features we need and employs exactly the same model potential as used in our global geometry optimisations. The standard velocity Verlet algorithm [46] was used for translational motion and a velocity Verlet-like algorithm (described in detail in ref. [47]) for rotational motion. The aim of our MD simulations was twofold: investigation of general structural stability of many of our clusters at various temperatures and detailed comparisons of dissociation behaviour of different structures near magic number sizes. For the first purpose, we implemented the Anderson thermostat ([54] and references therein). For the second purpose, we additionally implemented constrained dynamics, to enforce the target reactions within short simulation times and calculate free energies of dissociation easily. Following standard procedures described in detail in refs. [48–50], a given reaction path is followed stepwise by imposing constraints at each step, using Lagrangian multipliers and the RATTLE scheme [51]. The average constraint force $\langle F \rangle$ at each step can be calculated directly from these Lagrangian multipliers. Integration of the force as a function of the distance along the reaction path then yields the free energy ΔG. As a first example, we focus on the dissociation of single water molecules, which also has the advantage of making this procedure particularly simple.

3 Results and discussion

For the systems $M^+(H_2O)_n$, where M = Na, K, Cs, and for each value of n in the range $3 \leq n \leq 25$ we have performed at least eight global optimisation runs, in special cases up to 60. Most of the raw results and some of their interpretation have already been published elsewhere [27,54]. For completeness and easy reference we briefly summarise the central parts of these findings here. We then give a new analysis and interpretation of these results which will turn out to be of central relevance to the dynamics and the issue of magic numbers. This will be followed by a detailed discussion of characteristic dynamics of the investigated structures in Sect. 3.1.2.

3.1 Global minima for various cluster sizes

An extensive global geometry optimisation study has been performed for the alkali cation microsolvation clusters $M^+(H_2O)_n$, with M = Na, K, Cs, and reasons have been provided for the structural trends observed in refs. [27,52,54]. A detailed set of structural data can be found in references [27,54] whereas coordinate files and energy values of all global minima and many low-energy local minima are available from the authors upon request. A suitable basis for explanation of many structural features is an analysis of orientation-dependent pair interactions, as given in detail in refs. [27,54].

This analysis shows that the decisive feature is a delicate balance between optimal orientation of water molecules towards the cation, which makes it difficult for these water molecules to form hydrogen bonds with neighbouring water molecules, and optimal orientation of water molecules for hydrogen bonding, which leaves them in a less-than-optimal orientation towards the cation. The size of the cation then determines the energy cost for re-orientation of first- and second shell water molecules and thus determines whether this balance tips one way or the other. From this, all the observed structural trends can be explained.

The sodium cation is small and hence has a strong and far-reaching orientational influence on the surrounding water molecules. At least in smaller clusters, this cannot be compensated by the formation of a sufficient number of hydrogen bonds. Therefore, water network cages are not preferred around a sodium cation; in particular, the dodecahedron local minimum at $n = 20$ is not even of low energy. Instead, two other structural principles dominate: either the sodium cation sits in the centre of the cluster, with most of the water molecules oriented towards it, or it takes an off-centre position, with most of the water molecules forming a network around a first-shell water molecule. Direct competition between these two structural principles prevents obvious shell closures in any of them. This constitutes an explanation for the completely missing magic numbers in the sodium case [36].

The caesium cation is much larger. Therefore, even in its first shell non-optimal orientations of water molecules towards the cation are easily compensated by hydrogen bond formation. Hence, it is no surprise that even in the smallest clusters water rings form. For growing clusters, the water rings do not grow significantly, but rather four-, five- and six-membered rings join up. This can be interpreted as an optimisation of the balance between maximising the number of hydrogen bonds and minimising the ring strain. This tendency naturally leads towards clathrate-like cage structures.

Table 1 Numbers and types of different molecules present in the global minimum structures of $M^+(H_2O)_n$, M = Na, K, Cs (see text for explanation of the categorisation)

n	4	5	6	7	8	9	10	11	12	13	14	15	16	17	18	19	20	21
$Na^+(H_2O)_n$																		
Single	4	5	–	1	1	1	–	1	–	–	–	–	–	–	–	–	–	–
A	–	–	–	–	–	–	–	–	–	–	–	–	–	–	–	–	–	–
D	–	–	4	4	3	2	2	2	2	–	–	–	–	–	–	–	–	2
DA	–	–	–	–	1	1	2	1	1	1	–	1	1	1	1	2	1	–
AA	–	–	2	1	–	–	–	–	–	–	–	–	–	–	–	–	–	–
DD	–	–	–	–	–	–	–	1	1	2	–	2	1	2	2	2	2	1
DDA	–	–	–	–	–	1	2	1	2	3	7	4	6	5	3	4	5	4
DAA	–	–	–	–	3	4	4	5	6	7	7	8	8	9	8	8	9	9
DDAA	–	–	–	–	–	–	–	–	–	–	–	–	–	–	3	3	3	4
$K^+(H_2O)_n$																		
Single	4	2	–	1	1	–	–	–	–	–	–	–	–	–	–	–	–	–
A	–	–	–	–	–	–	–	–	–	–	–	–	–	–	–	–	–	–
D	–	–	–	2	2	2	2	1	–	–	–	–	–	–	–	–	–	–
DA	–	2	4	2	3	3	2	3	4	3	–	1	–	1	–	1	–	–
AA	–	1	2	–	–	–	–	–	–	–	–	–	–	–	–	–	–	–
DD	–	–	–	–	–	–	–	–	–	–	–	–	–	–	–	–	–	–
DDA	–	–	–	–	–	1	2	3	4	5	7	7	8	8	9	9	10	9
DAA	–	–	–	2	2	3	4	4	4	5	7	7	8	8	9	9	10	11
DDAA	–	–	–	–	–	–	–	–	–	–	–	–	–	–	–	–	–	1
$Cs^+(H_2O)_n$																		
Single	–	–	2	–	–	–	–	–	–	–	–	–	–	–	–	–	–	–
A	–	1	–	–	–	–	–	–	–	–	–	–	–	–	–	–	–	–
D	–	1	–	–	1	–	–	–	–	–	–	–	–	–	–	–	–	–
DA	4	3	4	5	5	5	6	5	4	5	4	3	2	3	–	1	–	1
AA	–	–	–	–	–	–	–	–	–	–	–	–	–	–	–	–	–	–
DD	–	–	–	–	–	–	–	–	–	–	–	–	–	–	–	–	–	–
DDA	–	–	–	1	1	2	2	3	4	4	5	6	7	7	9	9	10	10
DAA	–	–	–	1	1	2	2	3	4	4	5	6	7	7	9	9	10	10
DDAA	–	–	–	–	–	–	–	–	–	–	–	–	–	–	–	–	–	–

The first closure of such a cage occurs at $n = 18$, which is a tempting explanation for this magic number. The dodecahedron may seem as a natural culmination point of this structural principle, since it consists of only five-membered rings. However, its actual realization is quite distorted, and other cage structures are effectively isoenergetic, which already limits the appeal of the dodecahedron hypothesis considerably.

The potassium cation is intermediate in size between sodium and caesium, and its structural preferences are also intermediate between these two. Smaller clusters are more similar to their sodium analogue, while larger ones are closer to the caesium cases. For $n = 16$ we see a cage closure, which again coincides with the first magic number. For $n = 20$, the global minimum has a dodecahedral cage, but is strongly distorted, and clearly non-dodecahedral minima are only 7 kJ/mol higher in energy.

These results constitute a first complete and systematic overview on structures of alkali cation microhydration cluster $M^+(H_2O)_n$, with M = Na, K, Cs and $4 \leq n \leq 24$, based on global optimisation studies. It is also the first unbiased check of the dodecahedron hypothesis. One might object that the results have been obtained merely using a model potential; however, a complete and systematic overview would not have been possible using any ab initio method. Comparisons to ab initio calculations and to experimental results (to be published) show that the structures are at least qualitatively correct.

3.1.1 Are magic numbers due to a special structural pattern?

A structural pattern that all magic number structures seem to have in common is that none of the global and most important local minimum cluster structures contain any water molecules which form less than three hydrogen bonds, i.e. only water molecules which at least either donate two hydrogen bridge bonds and accept one (DDA) or vice versa (DAA) are present. Generally, the abbreviation D shall denote donor, i.e. one D for each donating OH bond per water molecule, and the abbreviation A is used for acceptor, i.e. one A for each accepted OH bond per water molecule. Single water molecules form no hydrogen bonds with any of the other water molecules in the water network but are bound only to the central ion. One may argue that two-coordinated water molecules (and of course also one-coordinated or single water molecules) are less well bound to the water network and may hence be centres of dissociation or association. According to this assumption, four-coordinated water molecules would be even better than three-coordinated ones. However, it is rather hard to build a cluster with four-coordinated water molecules if the total number of water molecules is small and if due to a

four-coordinated water molecule other water molecules will have to be located in an unfavourable bonding situation or for that matter badly accommodate the central ion.

Table 1 is a summary of the numbers and types of water molecules present in global minimum structures of different cluster sizes for all three systems. Some explanations for why special coordination numbers are preferred and by which system have already been given in Sect. 3.1. This section adds a few observations from yet another angle.

In Table 1 the number and types of different molecules present in the global minimum structures of $Na^+(H_2O)_n$ are given. The structure found for $Na^+(H_2O)_{14}$ is the only one which fulfils the above-mentioned criterion of three-coordinated molecules, but this cluster size is not known to be a magic number. However, contrary to the local minimum structures found for magic numbers which also show the same structural patterns in the case of $Na^+(H_2O)_{14}$ no other local minimum structure shows this feature. With this single exception, all cluster sizes have at least one water molecule with less than three hydrogen bonds. This nicely matches the experimental observation of completely missing magic numbers for sodium cation microhydration clusters.

Looking at the corresponding data for $K^+(H_2O)_n$ (see Table 1) the picture becomes different. In contrast to smaller cluster sizes (which exhibit a similar bonding pattern as $Na^+(H_2O)_n$, see Sect. 3.1), starting from $n = 14$, medium and larger cluster sizes seem to prefer an equal number of DDA and DAA molecules for an even total number of water molecules, whereas odd total numbers of water molecules have an additional DA molecule.

For $Cs^+(H_2O)_n$-clusters the case is yet again a little different. While $K^+(H_2O)_n$-clusters show an equal number of DDAs and DAAs starting from medium-sized clusters, $Cs^+(H_2O)_n$-clusters do this right from the beginning, where the first DDA and DAA molecules are present (see Table 1). For smaller cluster sizes, DA molecules can be found in every structure; nevertheless, they start to disappear again for even numbers, from $n = 18$, which is also the first magic number for $Cs^+(H_2O)_n$. In the experiment also 20, 22, 24 were found to be magic, again matching our simple DA count. In the case of $Cs^+(H_2O)_n$ the categorisation of magic numbers being due to only DDA or DAA molecules present in the structure at first sight seems to hold and also gives a reason for magic numbers starting at 18.

For all the three cations the most important local minima were checked upon in view of this criterion, and it was found that the categorisation still holds. However, no further information will be given in this work in order not to clutter it with too much data.

The exclusive presence of three-coordinated molecules may indeed be a good criterion for magic numbers in the size range under study. Exclusive three coordination also is clearly linked to (bent) two-dimensional rather than one-dimensional or three-dimensional water networks, and hence to water cages around a central ion. However, three-coordinated water molecules can form many sorts of cages, not only those consisting of five-membered rings, but also others containing four- and six-membered rings. Therefore this criterion extends the dodecahedral clathrate hypothesis in a simple but effective way.

3.1.2 Dynamics of $M^+(H_2O)_n$ with M = Na, K, Cs and $4 \leq n \leq 21$ using a canonical ensemble

For all three systems, i.e. $M^+(H_2O)_n$ with M = Na, K, Cs and $4 \leq n \leq 21$, molecular dynamics simulations were run using a canonical ensemble at four different temperatures: $T = 40$, 80, 120 and 150 K. These temperatures were selected since experiments such as mass spectrometry and infrared spectroscopy are assumed to be within this temperature region. As already explained in ref. [54], global geometry optimisation methods yield not only the global minimum structure in practice, but also extensive lists of low-energy local minimum structures. Using all these as starting structures for MD simulations gives an impression of the dynamics in regions of configuration space that are likely to be most relevant in dynamics studies, without expending the effort of full MD. However, due to time constraints, merely global minimum structures were used as input geometries here and just six runs (with a total simulation time of 10 ps and a time-step of 0.1 fs each) per structure and temperature could be performed. This does by no means represent a sufficient statistic, especially as no runs with local minimum structures as input were computed, except for the special case of $n = 20$ (see Sect. 3.1.6). Nevertheless, the obtained results still serve as a first guidance concerning trends in the dynamics of the water network. Again only a central subset of data is represented here, highlighting the most important points, while a full set of results for all n can be found in ref. [54].

For displaying all cluster structures in this work the program *xmakemol* [37] has been used. As this program has its own way to show interactions between particles some general remarks are in order, i.e. this program shows bonds for interactions between particles which should not always be mistaken for "real" bonds. In case of alkali cation microhydration clusters, these "bonds" concern water (oxygen)–cation and water (oxygen)–water (hydrogen), i.e. hydrogen bonds, interactions. The maximal length of these "bonds" can be manually adjusted by the user; however, the initial values the program uses are accepted standard values, hence these initial values were also adopted without further readjustment for depicting structures in this work. In the course of this work the term "bond breaking" hence will refer to the bonds which are no longer depicted by *xmakemol* due to an increased distance between two or more particles. Vice versa, if "bond formations" are mentioned this refers to a decreased distance between two or more particles.

3.1.3 $Na^+(H_2O)_n$

In summary, as expected, with rising temperature the movements of the molecules become stronger. At $T = 40$ K, mostly hindered rotational motion of molecules is observable and only small hindered translational movements for

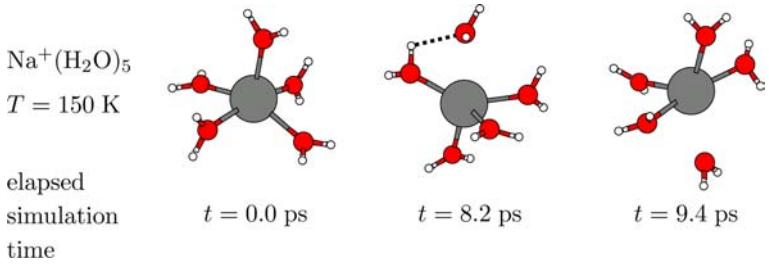

Fig. 1 Snapshots from the molecular dynamics simulation of $Na^+(H_2O)_5$ using a canonical ensemble at $T = 150$ K

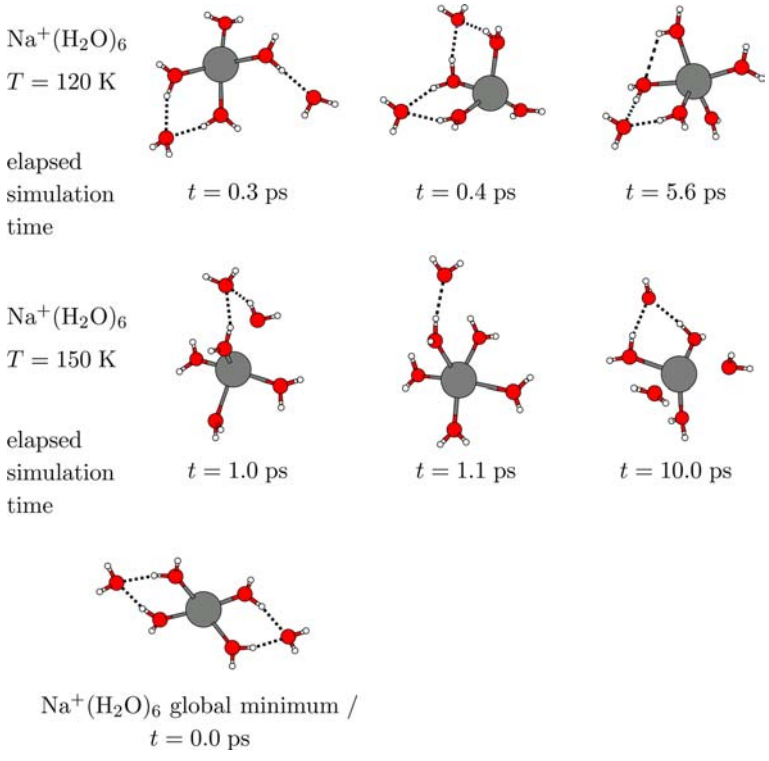

Fig. 2 Snapshots from the molecular dynamics simulation of $Na^+(H_2O)_6$ using a canonical ensemble and $Na^+(H_2O)_6$ (global minimum) as input geometry (see *bottom*) at $T = 120$ K and $T = 150$ K

some water molecules, mostly those sitting on the edge of a water network, thus being not as tightly "bound" by other water molecules. For $T = 80$ K the rotational motion is still more intense than the translational motion, though the translational motion becomes stronger. Due to the more intense movements, in some of the medium-to larger-sized cluster structures hydrogen bonds in the water network start to open up, but are closed again almost instantly. Also in the larger clusters, water molecules which are on the edge of the water network start to move back and forth between their original position and a position from where they can participate more strongly in the water network. All these movements still happen rather slowly. Hence no examples shall be depicted for these temperatures.

There is a qualitative change in behaviour between the temperatures $T = 80$ K and $T = 120$ K, as at $T = 120$ K the motion of the water molecules becomes a lot stronger and some cluster structures, mostly smaller sized ones, start to change. The larger clusters are less affected by the temperature rise, as most of the water molecules take part in an optimised and rather cohesive water network which hinders both their translational and rotational motions. Also, more simply, the total kinetic energy is distributed over many more degrees of freedom, resulting in less energy available in each of them. Combined with the fact that almost no changes are observable at $T = 40$ K, this strongly suggests that global geometry optimisation indeed produces structures which are relevant in the experiment.

Upon increasing the temperature to $T = 150$ K, the trend already observed for $T = 120$ K becomes more pronounced. Smaller clusters now readily change their structure and some larger cluster structures also open up, although the tendency to exhibit a compact water network still prevails. For more detailed examples see below. All this does not mean that these temperatures are insufficient to induce changes in any of those clusters. On the contrary in Sect. 3.1.6 we will show an

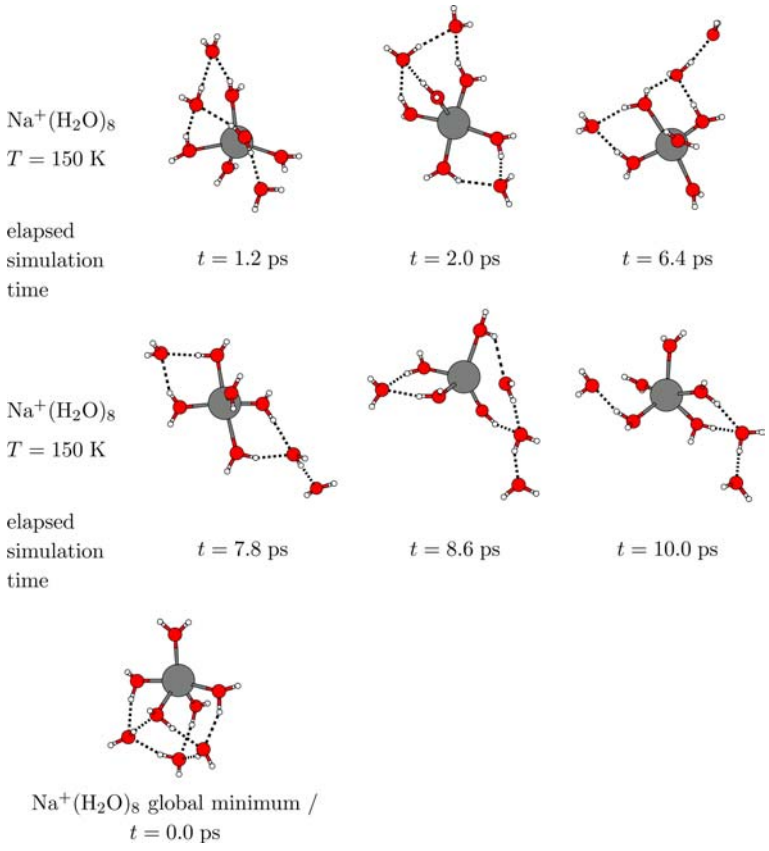

Fig. 3 Snapshots from the molecular dynamics simulation of $Na^+(H_2O)_8$ using a canonical ensemble and $Na^+(H_2O)_8$ (global minimum) as input geometry (see *bottom*) at $T = 150$ K

example where a large cluster structure undergoes a qualitative change easily and rapidly. Therefore the negative findings reported here really are an indication of stability.

In the case of $Na^+(H_2O)_4$, within our limited statistics no qualitative change in structure can be observed for any of the temperatures used in the simulation. The case of $Na^+(H_2O)_5$ is quite similar for temperatures up to $T = 120$ K, i.e. the structure stays more or less a distorted pyramid. For $T = 150$ K the pyramid starts to break up (see Fig. 1), changing between pyramidal and other structures. As there are still only five water molecules present, the variety of different cluster structures is still comparatively small. This structural variety increases a lot, when going for instance to $n = 6$ (see Fig. 2) or $n = 8$ (see Fig. 3). $Na^+(H_2O)_6$ already shows significant structural changes at $T = 120$ K. The rate of these changes increases for $T = 150$ K. In Fig. 2, snapshots of both temperatures are depicted. When looking at the actual movie at $T = 150$ K, the water molecules seem to wander around the ion, thus participating in somewhat similar or even equivalent structures at another position than before.

For structures around approximately $8 \leq n \leq 12$, the largest structural variety can be found. This is most probably due to the fact that with these numbers of water molecules no cohesive water network can yet be established and also due to the number of degrees of freedom still being moderate such that the available energy cannot be distributed over the network as extensively as for larger cluster sizes. It is important to note that no boundary box was implemented in the algorithm, hence leaving water molecules the possibility to completely dissociate from the cluster. One might expect this to happen for smaller clusters, as the water molecules are not yet connected by a cohesive water network. Nevertheless, not a single dissociation event was observed in any of our simulations. For cluster sizes of $8 \leq n \leq 12$, the coordination number of 5 is favoured for $5 \leq n \leq 8$, which can be seen in both Fig. 2 for $n = 6$ where the simulation starts with a (4+2) structure and proceeds onto different $(5 + 1)$ structures and Fig. 3 for $n = 8$ where the simulation is started with a $(5+3)$ structure, varieties of which can be seen throughout the simulation. Cluster sizes of $9 \leq n \leq 12$ prefer the coordination number 6. Hence, for numbers such as $5 \leq n \leq 8$, rather more hydrogen bonds to water molecules arranged in a second-shell are formed instead of forming structures with the coordination number 6 (see also ref. [54] for pair interactions of water molecules in different shells).

Moving on from $n = 8$ to $n = 15$ (see Fig. 4) and larger clusters, the cluster structures start to build up a cohesive water network on one side of the ion. This is typical for $Na^+(H_2O)_n$ as already explained in Sect. 3.1. For higher temperatures, such as $T = 120$ K and $T = 150$ K, hydrogen

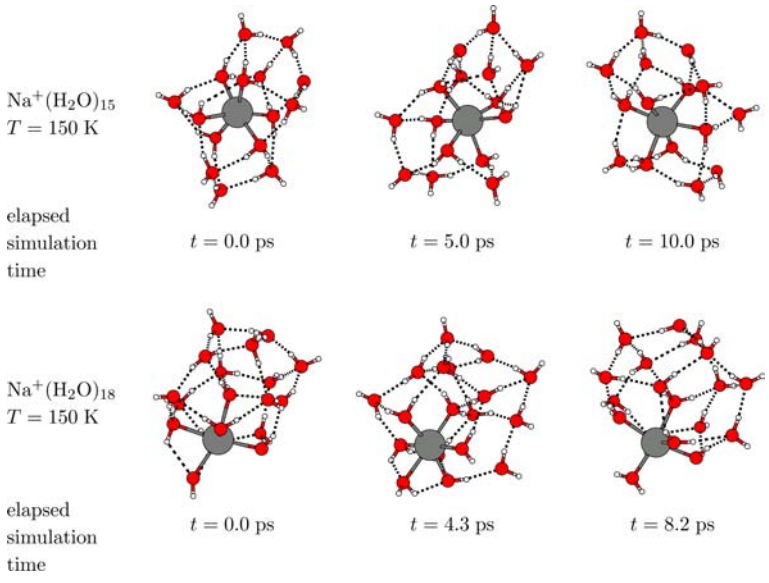

Fig. 4 Snapshots from the molecular dynamics simulation of $Na^+(H_2O)_{15}$ and $Na^+(H_2O)_{18}$ using a canonical ensemble at $T = 150$ K

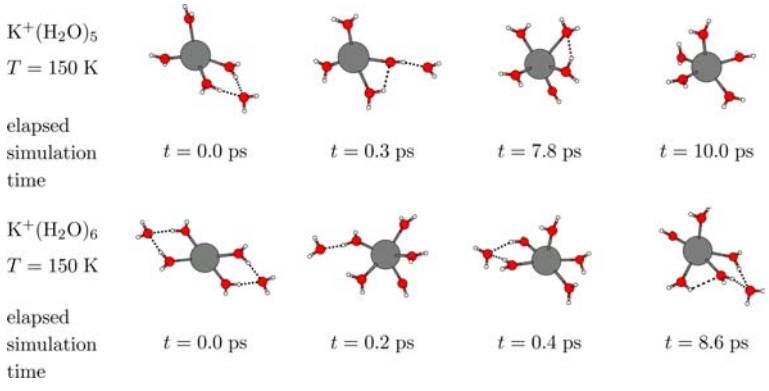

Fig. 5 Snapshots from the molecular dynamics simulation of $K^+(H_2O)_5$ and $K^+(H_2O)_6$ using a canonical ensemble at $T = 150$ K

bonds are still broken from time to time, but the water molecules then tend to move back to their original positions. Water molecules at the "edge" of the water network move back and forth between positions where they can take an active part in the network with more than just one hydrogen bond and where the ion attains its preferred coordination geometry. In Fig. 4, an example is given for $n = 18$. The simulation is started with a cluster structure where the water molecule at the open side of the ion participates with only one hydrogen bond in the water network. At a simulation time of $t = 4.3$ ps a snapshot is depicted where this molecule forms two hydrogen bonds with the rest of the water network, while at $t = 8.2$ ps it forms no hydrogen bonds thus momentarily resulting in an almost perfect octahedral shaped first shell of water molecules.

3.1.4 $K^+(H_2O)_n$

In most aspects small $K^+(H_2O)_n$ clusters behave similarly to $Na^+(H_2O)_n$ clusters so we focus on the differences here. For $K^+(H_2O)_5$, a (4+1) structure has been found as global minimum. Upon increasing the temperature to $T = 120$ K, this structure no longer seems to be the preferred one (see Fig. 5). Rather a coordination number of 5 is favoured, similar to the structures found for $Na^+(H_2O)_5$ which is most probably due to an entropy effect as $(4 + 1)$ is more rigid than $(5 + 0)$.

Advancing to $n = 7$, the choice of the coordination number 5 still seems to be in favour for $T = 80$ K and $T = 120$ K, though for $T = 150$ K the coordination number 6 can be found more often (see Fig. 6). Nevertheless, a clear preference of certain coordination numbers is less pronounced for the potassium case. For $K^+(H_2O)_n$ the structural variety is probably largest for $7 \leq n \leq 9$.

For cluster sizes around $9 \leq n \leq 14$, potassium cluster structures do not seem to be able to decide whether they should start preferring annealed rings or follow the path of sodium clusters. This trend of potassium taking an intermediate position between sodium and caesium clusters has already been explained for static structures in Sect. 3.1. As an example, Fig. 7 depicts the case of $n = 10$: the simulation is started

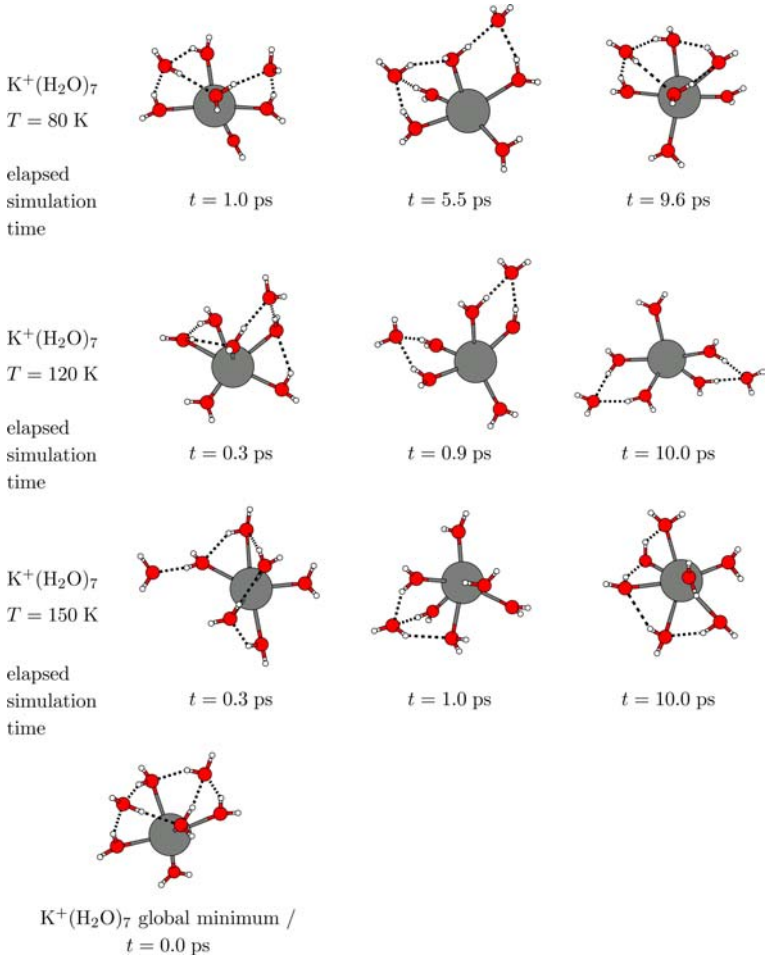

Fig. 6 Snapshots from the molecular dynamics simulation of $K^+(H_2O)_7$ using a canonical ensemble and $K^+(H_2O)_7$ global minimum as input geometry (see *bottom*) at $T = 80$ K, $T = 120$ K and $T = 150$ K

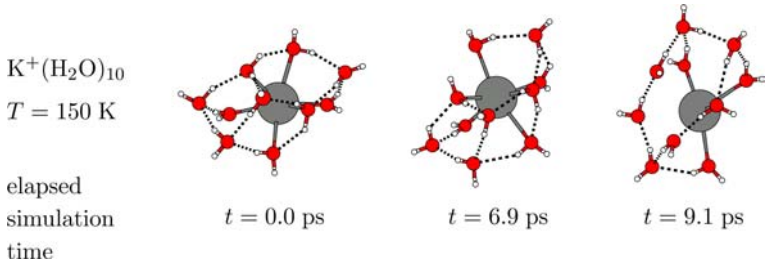

Fig. 7 Snapshots from the molecular dynamics simulation of $K^+(H_2O)_{10}$ using a canonical ensemble at $T = 150$ K

with a structure that mostly contains annealed rings which are then broken apart during the simulation, as depicted for $t = 6.9$ ps and $t = 9.1$ ps, while in between the cluster tries to re-form new annealed rings.

For cluster sizes with $n \geq 16$, potassium clusters behave more like caesium clusters, i.e. preferring annealed rings over more open structures. Looking at the dynamics of these cluster sizes, the water network more or less keeps its shape, occasionally opening and closing one or the other hydrogen bond (see Fig. 8). $n = 16$ happens to be a magic number for $K^+(H_2O)_n$ and in Sect. 3.1 it was assumed that maybe this magic number is due to a shell closure, thus exhibiting a stronger water network compared to its smaller and larger relatives. In Sect. 3.1.1 it was additionally speculated that magic numbers might be due to a structural pattern that all magic numbers seem to have in common, namely exhibiting only water molecules which have a coordination number of either 3 or 4. Hence the dynamics of $K^+(H_2O)_{16}$ were compared to that of its immediate neighbours, $K^+(H_2O)_{15}$ and $K^+(H_2O)_{17}$, bearing this pattern in mind. Although DA molecules seem to be able to move more freely, as they are only bound to two other water molecules, so far no significant

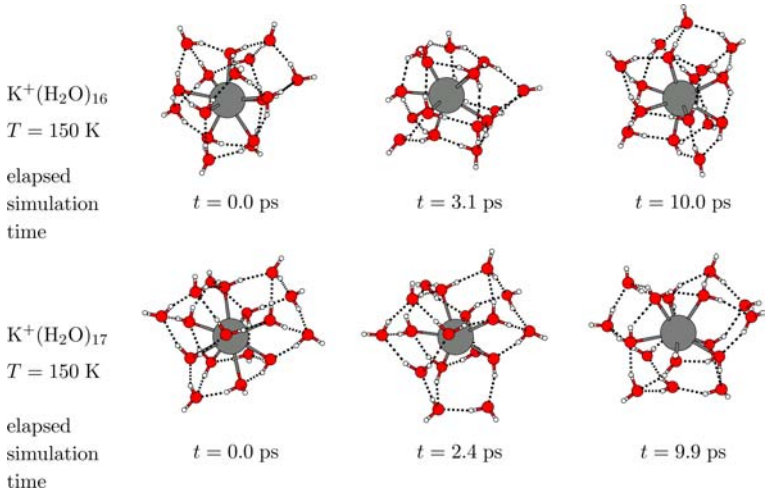

Fig. 8 Snapshots from the molecular dynamics simulation of $K^+(H_2O)_{16}$ and $K^+(H_2O)_{17}$ using a canonical ensemble at $T = 150$ K

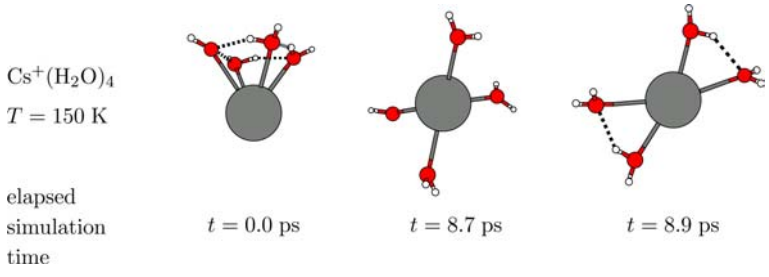

Fig. 9 Snapshots from the molecular dynamics simulation of $Cs^+(H_2O)_4$ using a canonical ensemble and $Cs^+(H_2O)_4$ (global minimum) as input geometry at $T = 150$ K

difference between the behaviours of the respective cluster hulls could be found. Possibly, significant differences could be found by the constrained dynamics technique used in Sect. 3.1.7 to examine the magic number 20. But then $n = 16$ is only a very weak magic number. Therefore this topic shall not be explored any further at this stage. The more important magic number, $n = 20$, is treated in a separate Sect. (see Sect. 3.1.6).

3.1.5 $Cs^+(H_2O)_n$

In some, though not all, aspects the dynamics of $Cs^+(H_2O)_n$ is comparable to the dynamics of both $Na^+(H_2O)_n$ and $K^+(H_2O)_n$: the greatest number of changes in cluster structure and simultaneously the most serious changes are observed for small cluster sizes, whereas the bigger the clusters get, the less pronounced the movements become. The movements for caesium cluster structures below $T = 80$ K are even less pronounced than those observed for potassium clusters. Unlike both potassium and sodium clusters, for caesium clusters no opening of any of the hydrogen bonds could be observed below $T = 80$ K. However, when increasing the temperature to $T = 120$ K movements become apparent and even more so for $T = 150$ K. The behaviour gap between $T = 80$ K and $T = 120$ K is quite outstanding for $Cs^+(H_2O)_n$, though it is also present for the other two systems in an alleviated form. As the gap becomes larger when increasing the mass of the ion, very simply the ion mass may be responsible. An ion as light as sodium can experience stronger movements at lower temperature than the caesium ion, which would in turn affect the water molecules.

For small cluster sizes, i.e. up to approximately $n = 10$, static $Cs^+(H_2O)_n$ cluster structures contain rings as early as possible compared to their relatives $Na^+(H_2O)_n$ and $K^+(H_2O)_n$. Looking at the dynamics of $Cs^+(H_2O)_4$ at $T = 120$ K and T=150 K (see Fig. 9), one observes that $Cs^+(H_2O)_4$ readily opens up its four-membered ring. In the course of the simulation, the tetrahedron seems to be the preferred structure, as after the ring opening the structures interchange between the structures depicted in Fig. 9 and the tetrahedron. As observed above for $K^+(H_2O)_n$, it is likely that this dynamical preference of a local minimum over a global minimum is an entropy effect.

Similar to $K^+(H_2O)_n$ with $9 \leq n \leq 14$, $Cs^+(H_2O)_7$ dynamics visit both open structures and structures where annealed rings are formed. Figure 10 shows snapshots from a typical trajectory, with different ring patterns being formed and destroyed again. Most of the time, however, at least one four- or five-membered ring is present; intervals with purely open structures are extremely short. In spite of these rearrangements at $T = 120$ K, compared to potassium clusters, caesium clusters still show their tendency to keep a large

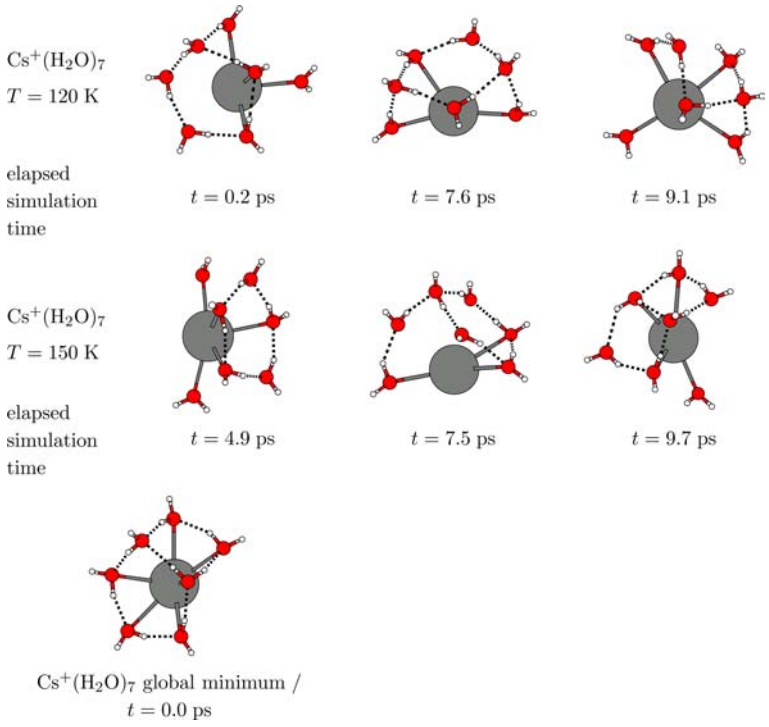

Fig. 10 Snapshots from the molecular dynamics simulation of $Cs^+(H_2O)_7$ using a canonical ensemble and $Cs^+(H_2O)_7$ global minimum as input geometry (see *left*) at $T = 120$ K and $T = 150$ K

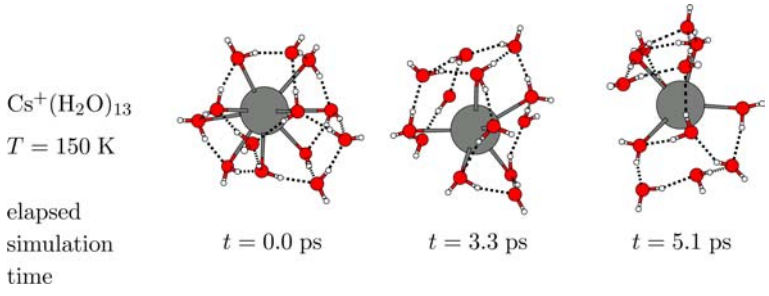

Fig. 11 Snapshots from the molecular dynamics simulation of $Cs^+(H_2O)_{13}$ using a canonical ensemble at $T = 150$ K

number of hydrogen bonds, sometimes resulting in a long chain of water molecules wrapped around the ion. This trend continues for $7 \leq n \leq 11$ although it becomes less pronounced for $9 \leq n \leq 11$ as the water network already forms one half of a shell surrounding the central ion.

Moving onwards to $n = 13$ (see Fig. 11), the cluster structures start to less readily open up for $T = 150$ K, as already found for $n = 11$ and $T = 120$ K. The snapshots depicted in Fig. 11 give a rare example of a simulation in which the cluster structure still breaks. However, it takes less than 1 ps after the break-up for the cluster structure to obtain a shape similar to the initial structure, as the coherence of the water network starts to become stronger. This trend continues for even larger systems.

Similar to $K^+(H_2O)_{16}$, a first shell closure is observed at $n = 18$ for the case of caesium (see Sect. 3.1), which again is a magic number. Comparing the dynamics of cluster structures with $17 \leq n \leq 19$, one observes that although the already rather cohesive water network hinders the movements of all three cluster sizes equivalently, cluster structures with $n = 18$ open up hydrogen bonds extremely seldom, even more seldom than $n = 17$ and $n = 19$. Though we only have a few representative trajectories, these findings indicate that $n = 18$ may be dynamically more stable than $n = 17$ and $n = 19$. In Fig. 12 an example is given of one of the rare occasions at $T = 150$ K where hydrogen bonds are indeal broken up for $Cs^+(H_2O)_{18}$, see snapshots at $t = 0.2$ ps and $t = 5.2$ ps. Obviously, the cluster structure does not change much qualitatively, in spite of the hydrogen bond breakings.

3.1.6 Dynamics of dodecahedral cage structures

As already mentioned in ref. [54], in case of $Cs^+(H_2O)_{20}$ the global minimum structure (dodecahedral) and the best non-dodecahedral structure are almost isoenergetic. The pair potential terms between the cation and all water molecules add

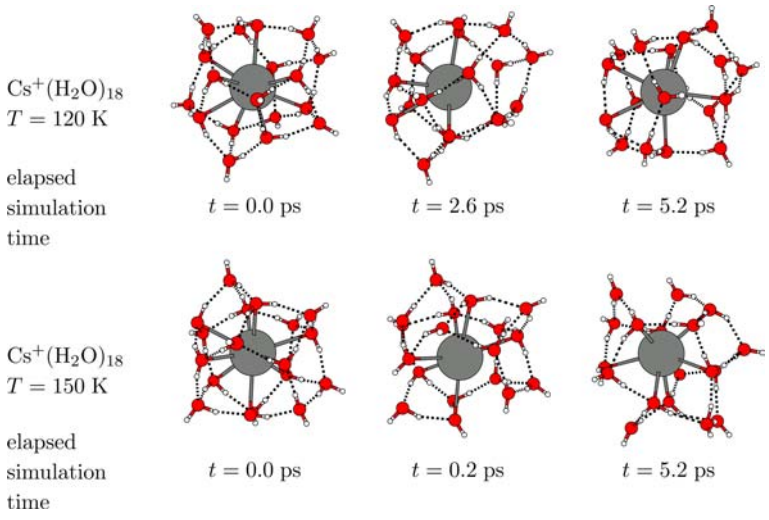

Fig. 12 Snapshots from the molecular dynamics simulation of $Cs^+(H_2O)_{18}$ using a canonical ensemble at $T = 120$ K and $T = 150$ K

up to 399.65 kJ/mol for the dodecahedron and 403.29 kJ/mol for the non-dodecahedron. Hence, the water network contributions appear to be better for the dodecahedral-like cage. However, this just barely over-compensates the better embedding of the ion in the non-dodecahedral cage structure to a final difference of not even 1 kJ/mol. As stated in ref. [54], a water hull consisting only of five-membered rings may have a kinetic advantage: it is speculated that sequential ring enlargement may be a preferred mode of water cluster growth, as seen in the experimental environment of helium droplets [55]. Also, for the pure water hexamer, a single six-membered ring is energetically less favourable than two annealed four-membered rings. Therefore, the dodecahedron may form a natural culmination point. Hence, both structures (dodecahedral and non-dodecahedral) were submitted to cluster dynamics using a canonical ensemble and also to constrained dynamics in order to evaluate the free energy of the dissociation of single water molecules from both water hulls (see following section). For comparison, canonical ensemble dynamics were also computed for $K^+(H_2O)_{20}$ and $Na^+(H_2O)_{20}$ (see below).

When comparing the dynamics of both structures of $Cs^+(H_2O)_{20}$, no difference whatsoever could be observed for temperatures $T = 40$ K, $T = 80$ K and $T = 120$ K, respectively. Rather, both structures follow the trends given in Sect. 3.1.2, namely no changes occur apart from small hindered rotational motion and even smaller hindered translational motion of individual molecules. When increasing the temperature to $T = 150$ K, again for the dodecahedron structure not even a single hydrogen bond opening could be observed, though the water molecules wiggle around a little more. This does not necessarily mean that bond openings do not occur at all for the dodecahedral structures as due to limited disk space not each time-step was recorded for the analysis. However, it is assumed that according to statistics at least one or two bond openings should have been visible in at least one of the movies. For the non-dodecahedral cage structure occasional bond openings between two annealed four- and six-membered rings were observed. Hence this might be a weak indication that indeed the overall dynamical stability of the dodecahedron structure is slightly better compared to that of a non-dodecahedron. However, to us this is not a convincing explanation for the magic number status of $n = 20$.

For $K^+(H_2O)_{20}$, the global minimum is also a dodecahedron-shaped cluster structure [54]. Both the global minimum structure and the best non-dodecahedral structure were submitted to molecular dynamics simulation. Again, for $T = 40$ K and $T = 80$ K, apart from rotational and small translational motions nothing of importance occurs. For $T = 120$ K and $T = 150$ K occasional hydrogen bond openings were observed for both cluster structures. Hence from just comparing the dynamics of the two different structures no further insight into the status of the dodecahedron hypothesis could be gained in the case of $K^+(H_2O)_{20}$.

In the case of $Na^+(H_2O)_{20}$, the dynamics of a constructed and locally optimised dodecahedron-shaped structure (see ref. [54]) was compared to that of the global minimum structure. As already explained in Sect. 3.1.2, for $T = 40$ K and $T = 80$ K apart from very small rotational and even smaller translational motions nothing much occurs in the case of the global minimum structure. Even when increasing the temperature to $T = 120$ K or $T = 150$ K, the water molecules of the water network only wiggle around their initial positions whereas the water molecules on the edges move between positions where they take up an active part in the water network and positions that allow the sodium ion to have its preferred coordination geometry. Overall the cluster structure stays the same and does not change its general appearance during the simulation.

However, the behaviour of the dodecahedron-shaped water hull is different. Starting with temperatures of $T = 80$ K, the static local minimum dodecahedron structure of $Na^+(H_2O)_{20}$ is extremely distorted, as the sodium ion is simply too small to fill the cage. Hence the ion clings

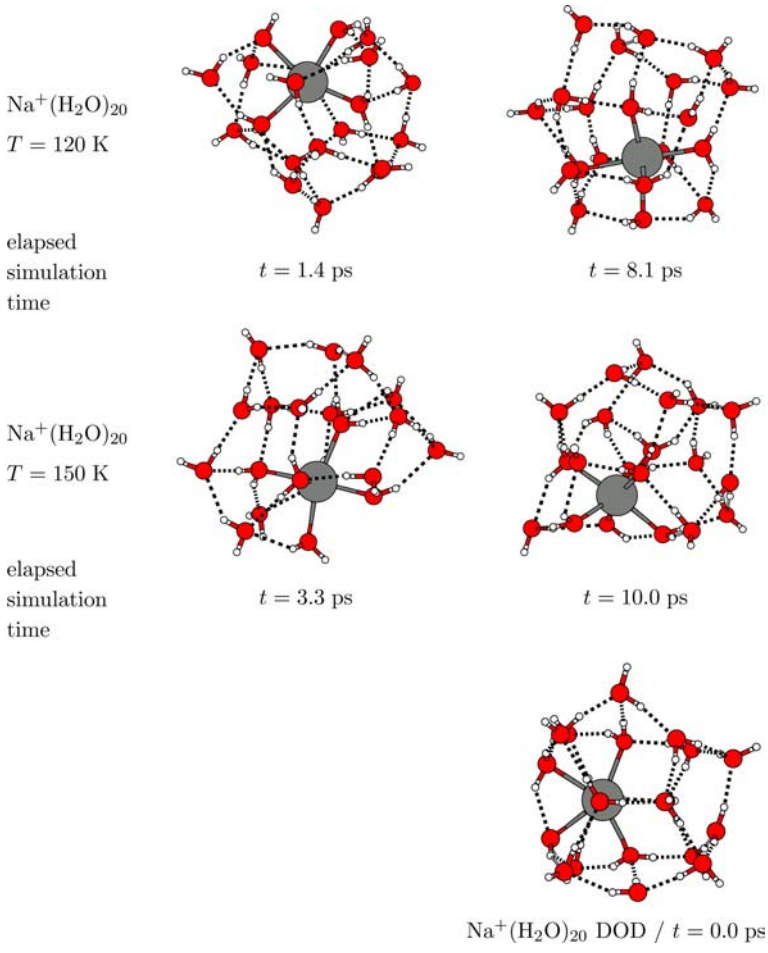

Fig. 13 Snapshots from the molecular dynamics simulation of $Na^+(H_2O)_{20}$ using a canonical ensemble and $Na^+(H_2O)_{20}$ DOD as input geometry (see *bottom*) at $T = 120$ K and $T = 150$ K

to one side of the dodecahedron hull (see Fig. 13), which leaves it "open" to the other side. The number of water molecules arranged around the central ion in a first-shell is equal to 6, but due to the cage-like structure of the water network they cannot be arranged in an octahedron shape which is the preferred ion coordination geometry of the global minimum structures of $n \geq 17$. This implicates that one of the first-shell water molecules that is close to the "open side" of the ion will try to move into a position which fills the gap in the cage interior and allows the sodium ion to obtain an octahedral-shaped first-shell coordination geometry. And indeed this is found to be a general mechanism. While this change occurs the dodecahedron hull starts to break apart such that the water molecule is allowed to move to its preferred position while maintaining as many hydrogen bonds as possible. In other words, during the simulation the five-membered rings are broken apart and new rings are re-formed as soon as possible, though now also four- and six-membered ones, in order to lessen the strain on the water network. Upon increasing the temperature to $T = 120$ K and $T = 150$ K, these changes are advanced even further, until at $T = 150$ K the dodecahedron cluster structure arrives at a structure very similar to the global minimum structure by the end of the simulation. To ensure that this was not just plain coincidence, another 20 simulations were run on this special case which confirmed the findings: In all simulations performed, the dodecahedron-shaped structure changed, taking up forms which were equivalent or very close to the global minimum structure.

This is indeed a very surprising result as the MD simulations performed were just basic MD simulations, merely enforcing a canonical ensemble, but by no means forcing any structural transformations. Also these structural transformations do not just occur occasionally but very frequently. However, barrier crossings usually are very rare events in MD, hence one would not expect them to happen too frequently. Also, as the energy landscape of systems of this size is extremely complex, one would not expect the same transformation to happen in different trajectories. A possible explanation might be that the barriers are indeed relatively small, thus allowing frequent crossings of many structurally similar low-energy barriers to collectively form a simple deformation pathway connecting these two seemingly so different structures. Another view of basically the same situation postulates features of several different sizes on the energy landscape, e.g. a big funnel towards the global minimum on a large scale and on a smaller scale a large number of smaller

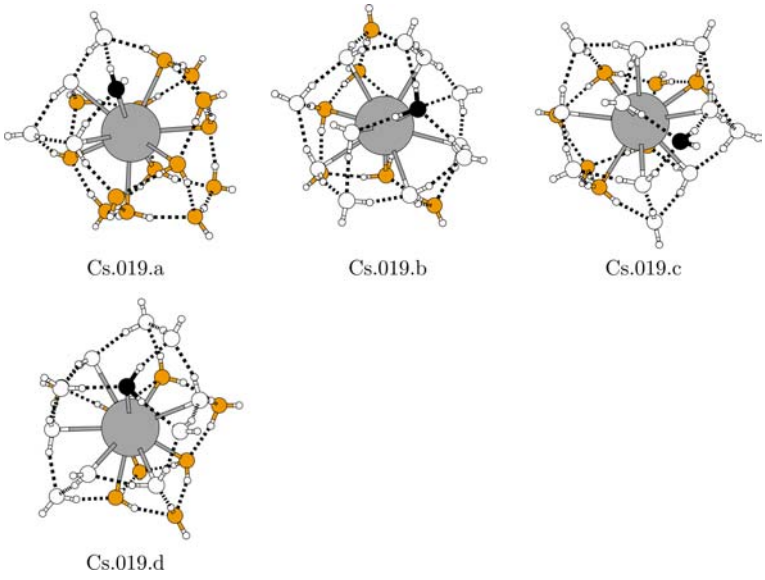

Fig. 14 Global minimum structure of $Cs^+(H_2O)_{19}$ where the water molecules marked *black* indicate the pulled water molecules whereas the *white* water molecules indicate annealed rings which contain the pulled water molecule

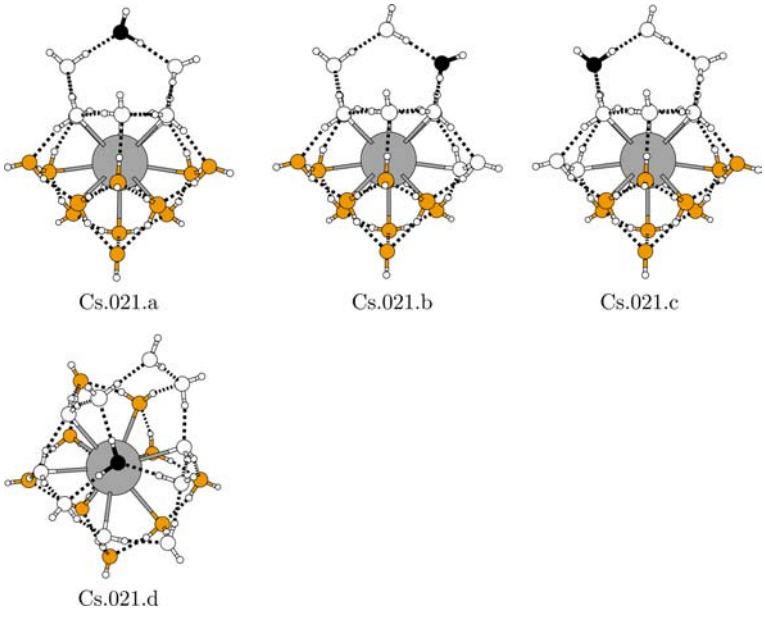

Fig. 15 Global minimum structure of $Cs^+(H_2O)_{21}$ where the water molecules marked *black* indicate the pulled water molecules whereas the *white* water molecules indicate annealed rings which contain the pulled water molecule

subminima of this structure which are only divided by low-energy barriers. Such a picture is often evoked to explain the comparatively rapid and reproducible transformation events of other large molecular assemblies, e.g. proteins [53]. In any case, these results clearly show that dodecahedral cages are not important for $Na^+(H_2O)_{20}$. Instead, a possibly large set of related structures similar to the off-centred, non-dodecahedral global minimum structure is preferred.

These findings are not only important as further support for an earlier explanation [36] for the non-existence of the magic number $n = 20$ in the case of $Na^+(H_2O)_n$, but also prove that indeed the use of quasistatic global geometry optimisation is justified as a tool to circumvent the effort and expenses of full molecular dynamics simulation, even for rather non-rigid systems.

3.1.7 Constrained dynamics

The magic number $n = 20$ is most prominent in the case of $Cs^+(H_2O)_{20}$, rather weak for $K^+(H_2O)_{20}$ and not observed to be a magic number for $Na^+(H_2O)_{20}$. The conclusion of the

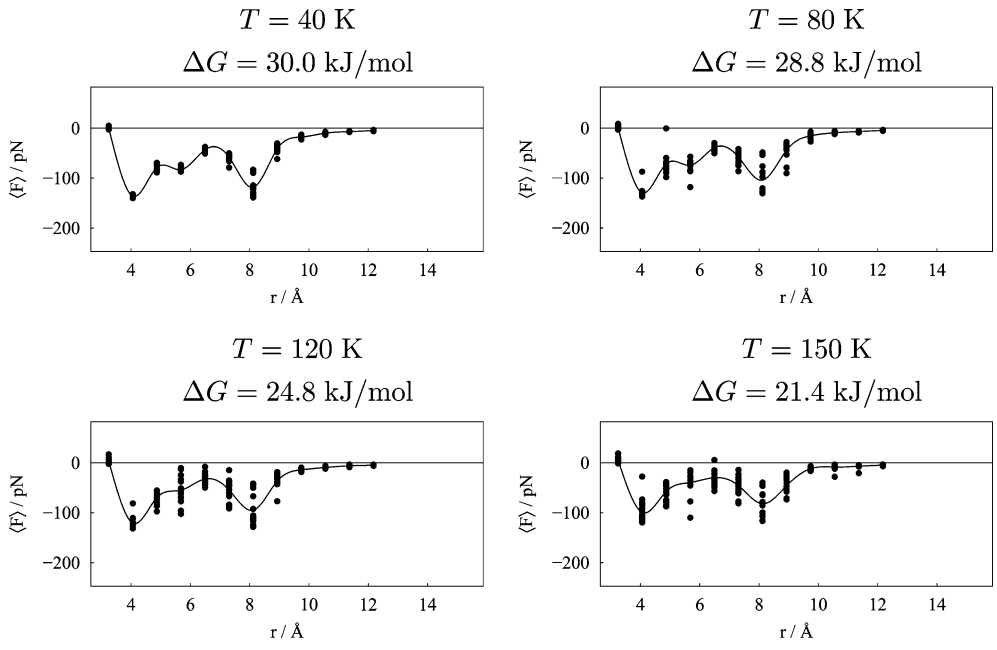

Fig. 16 Average constraint force $\langle F \rangle$ in pN vs. distance r in Ångström of pulled water molecules of structure $Cs^+(H_2O)_{19}$ (Cs.019.d) for 18 starting conditions per distance r each at T = 40 K, T = 80 K, T = 120 K and T = 150 K

previous section was that the sodium ion is simply too small for $Na^+(H_2O)_{20}$ to prefer a dodecahedron-shaped structure or for that matter any clathrate cage (see also ref. [54]). It was also indicated in ref. [54] that the potassium ion still seems a little too small for the dodecahedron cage, as it also prefers to be located somewhat off-centred. In contrast, the caesium ion rather perfectly fits a dodecahedral clathrate cage composed of 20 water molecules (although the cage is quite puckered). Therefore, this simple size-fitting argument still supports the dodecahedron hypothesis as a candidate explanation for magic numbers at $n = 20$. However, as already shown in ref. [27] and summarised here (see Sect. 3.1) several other non-dodecahedral structures are almost as good as the dodecahedral cages, for both K and Cs. For example, the best non-dodecahedral cage fits around the Cs cation just as well as the dodecahedral cage. This makes the dodecahedral hypothesis unlikely as far as static energetics are concerned. In the previous section, we have not found any significant differences in cage dynamics, using free canonical MD runs. However, it could still be possible that dodecahedral cages show enhanced dynamic stability against dissociation. Since we did not see any dissociation events at all in our free MD runs, we decided to enforce such reactions, using single molecule dissociations as prototype example. Also $Cs^+(H_2O)_{19}$ and $Cs^+(H_2O)_{21}$ were investigated, as may be the explanation for to why $n = 20$ is magic lies in the difference between the nearest neighbours of $Cs^+(H_2O)_{20}$ and itself.

Due to limited time, the free energy of the dissociation could not be computed for every molecule of each of the four structures, $Cs^+(H_2O)_{19}$, $Cs^+(H_2O)_{20}$ (dodecahedron/dod), $Cs^+(H_2O)_{20}$ (best non-dodecahedron/bnd) and $Cs^+(H_2O)_{21}$ hence water molecules were selected which are representative for several water molecules in similar surroundings (in ref. [54], we have shown that this generalisation is indeed possible). For $Cs^+(H_2O)_{19}$ and $Cs^+(H_2O)_{21}$, four water molecules were selected each. As one structural pattern all magic numbers have in common is that they do not contain water molecules which exhibit a coordination number smaller than three, see Sect. 3.1.1, the water molecule selected to be pulled from both $Cs^+(H_2O)_{19}$ and $Cs^+(H_2O)_{21}$ was a (or the) DA molecule. Two other likely candidates were its two adjacent molecules. The fourth molecule to be pulled from both structures was one that had a similar surrounding compared to the water molecules of both $Cs^+(H_2O)_{20}$ structures. For the corresponding structures of $Cs^+(H_2O)_{19}$ and $Cs^+(H_2O)_{21}$ see Figs. 14 and 15. For both the $Cs^+(H_2O)_{20}$ structures four DDA molecules and three DAA molecules were selected, respectively.

In Fig. 16, average force vs. distance plots are displayed for Cs.019.d at the four different temperatures $T = 40$ K, $T = 80$ K, $T = 120$ K, and $T = 150$ K respectively. Each point in one plot represents the average force computed from one of the 18 different starting conditions (hence a total of 198 simulations per plot were computed). The continuous curve is a spline interpolant. When looking at the four plots in Fig. 16, one observes that the overall form of the curve stays about the same, while maxima and minima become less pronounced for increasing temperatures. The free energy of the dissociation of one water molecule drops by 8.6 kJ/mol upon increasing the temperature from $T = 40$ K to $T = 150$ K, from $\Delta G = 30.0$ kJ/mol to $\Delta G = 21.4$ kJ/mol. Due to the fact that most structural changes appear to happen for temperatures $T \geq 120$ K and that no fundamental changes in the average force vs. distance plots can be observed for different

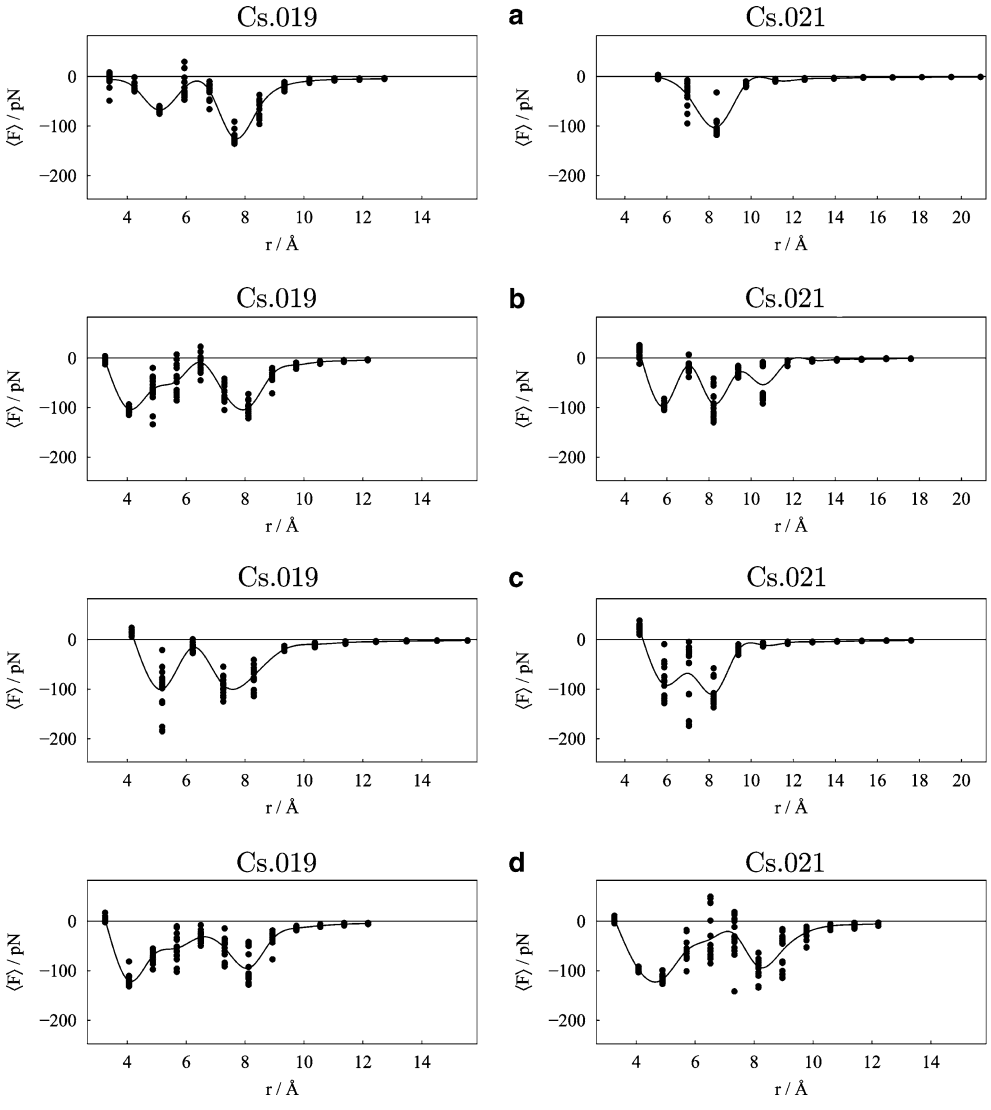

Fig. 17 Average constraint force $\langle F \rangle$ in pN vs. distance r in Ångström of pulled water molecules of structure $Cs^+(H_2O)_{19}$ and $Cs^+(H_2O)_{21}$ (for 18 starting conditions per distance r each) at $T = 120$ K

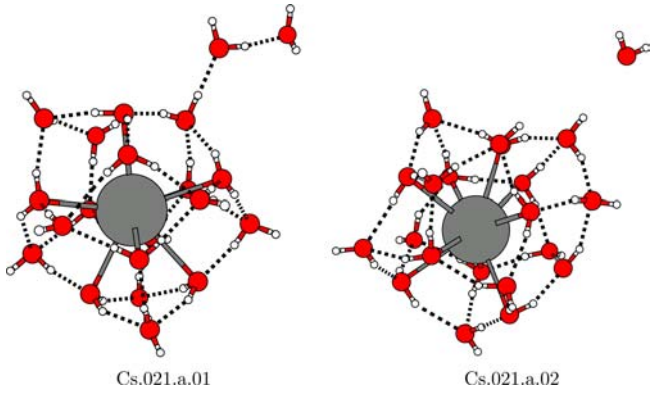

Fig. 18 Equilibrium structures of $Cs^+(H_2O)_{21}$ for two different starting conditions with a distance r of 8.3 Å for the constraint molecule at $T = 120$ K

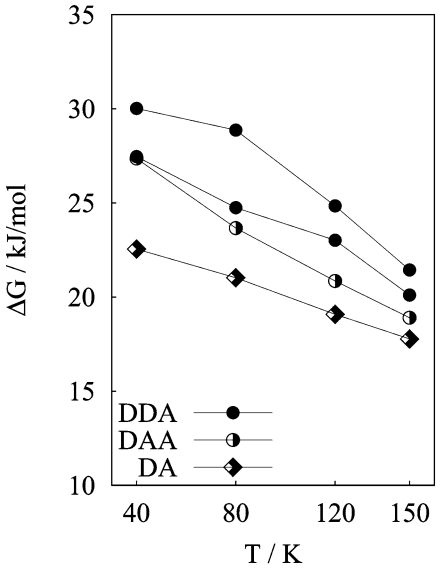

Free energies of water molecules pulled from $Cs^+(H_2O)_{19}$

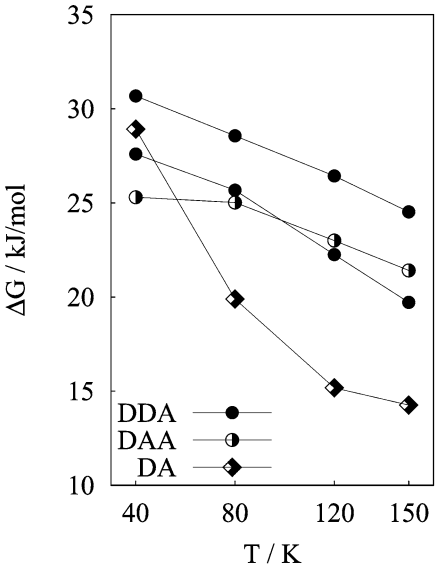

Free energies of water molecules pulled from $Cs^+(H_2O)_{21}$

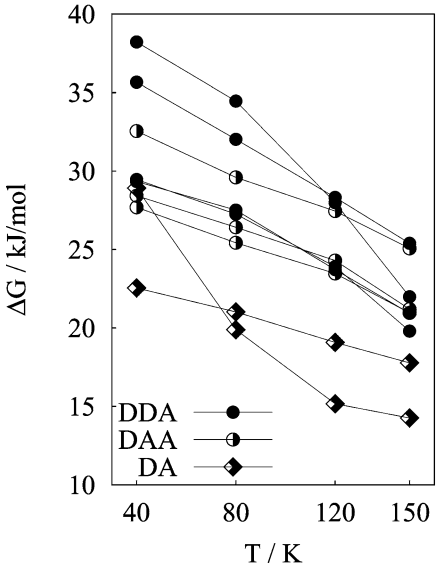

Free energies of water molecules pulled from $Cs^+(H_2O)_{20}$ (DOD) including the free energies obtained from pulling the DA-molecules from both $Cs^+(H_2O)_{19}$ and $Cs^+(H_2O)_{21}$ (see above)

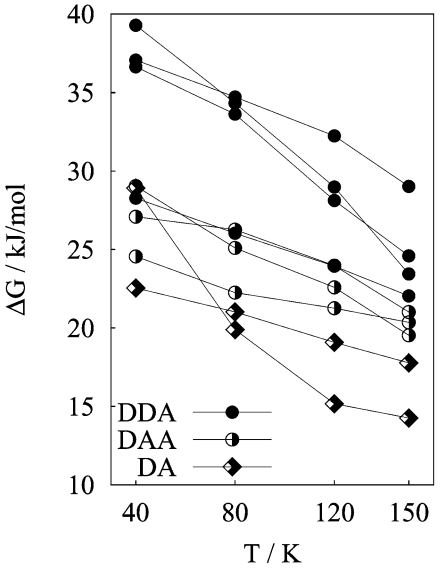

Free energies of water molecules pulled from $Cs^+(H_2O)_{20}$ (BND) including the free energies obtained from pulling the DA-molecules from both $Cs^+(H_2O)_{19}$ and $Cs^+(H_2O)_{21}$ (see above)

Fig. 19 Graphic representation of the free energies depicted in Table 2 (for further explanation see text)

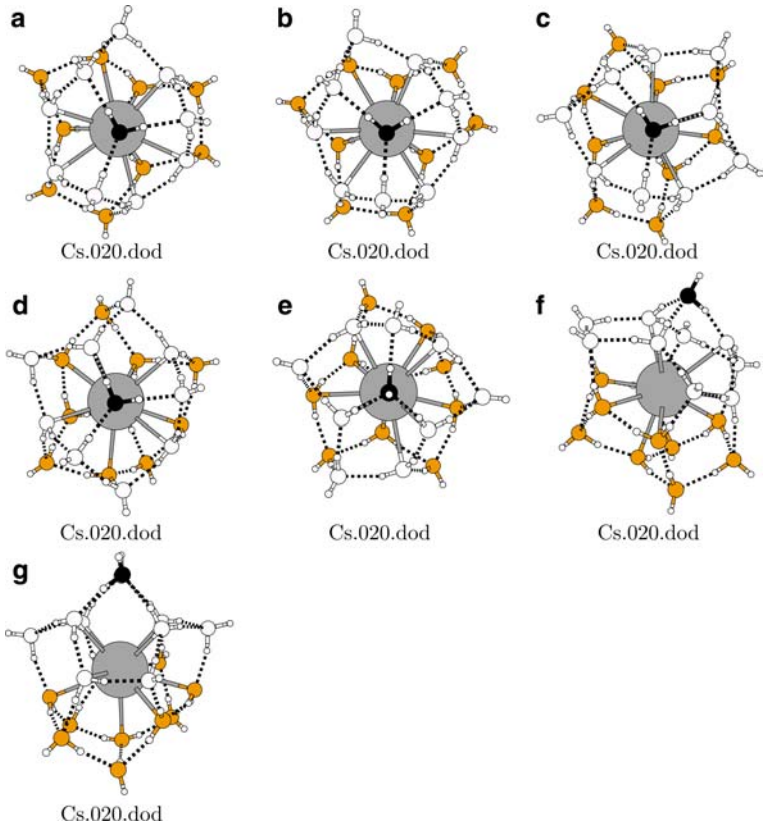

Fig. 20 Global minimum structure of $Cs^+(H_2O)_{20}$ (dodecahedral) where the water molecules marked *black* indicate the pulled water molecules whereas the *white* water molecules indicate annealed rings which contain the pulled water molecule

temperatures, in the course of this section only a selection of average force vs. distance plots at $T \geq 120\,\mathrm{K}$ will be described in detail [also for both $Cs^+(H_2O)_{20}$ structures], whereas a full set of plots for all structures and all temperatures can be found in ref. [54].

Minima in the average force vs. distance plots correspond to distances where the pulled water molecule occupies a position of optimal "hydration shell" distance to the central ion and simultaneously also to the other water molecules in the network. These distances approximately correspond to the optimal distances given in ref. [27,54] when looking at pair interactions. Average force vs. distance plots for all structures of $Cs^+(H_2O)_{19}$ and $Cs^+(H_2O)_{21}$ at $T = 120$ K are depicted in Fig. 17 as an example for the plots of these two structures.

Comparing the average force vs. distance plots of the same type of water molecule being pulled from the cluster such as for example Cs.019.c and Cs.021.c, which in both cases is a DAA molecule, one can observe subtle similarities between the plots, i.e. the trends of the curves are approximately the same, each exhibiting two minima and one maximum, though the amplitude of the extrema vary. When looking more closely at the surroundings of these two DAA molecules, one finds that they do not have an equivalent surrounding with respect to what types of water molecules donate or accept the hydrogen bonds. Comparing the average force vs. distance plots of the same type of water molecule exhibiting equivalent surroundings, such as Cs.019.d and Cs.021.d, one observes that both plots are indeed very similar and also yield similar free energies (see Table 2). Hence equivalent surroundings seem to be important for the actual comparison of values of the free energy of dissociation of one water molecule.

Another feature all plots have in common is that for larger distances of the pulled water molecule with respect to the central ion, the scatter of the points is smaller and vice versa. It was found that this scattering is due to different equilibrium structures obtained at the end of the simulation for the same input geometry but different starting conditions. See for example Fig. 18 where for Cs.021.a.01 the constrained water molecule is bound by one hydrogen bond to another water molecule which in turn is bound to the remaining water network, yielding an average force of -32.13 pN. For Cs.021.a.02, however, the constrained molecule does not have direct contact with the water network, while the water cage consists of a structure very close to that of the best non-dodecahedron for $Cs^+(H_2O)_{20}$ yielding an average force of -115.3 pN. In both cases the distance for the constrained molecule is equal to 8.3 Å. In case the difference between the two equilibrium structures is less pronounced, e.g. in case the constrained molecule can decide whether to function as a DDA or DAA in the water network, the average forces still scatter though not as strongly.

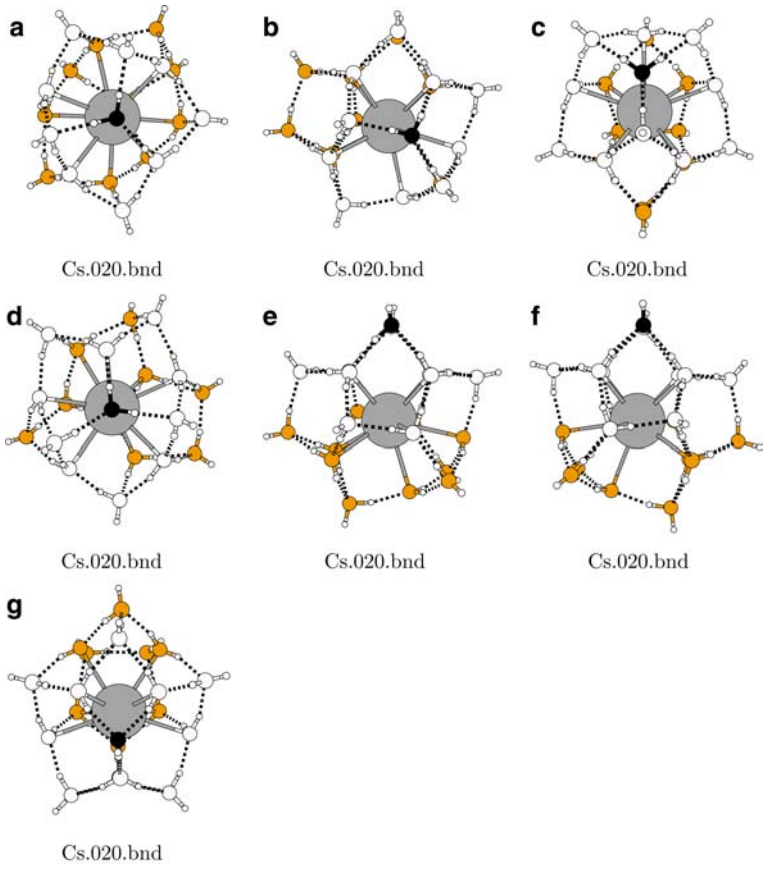

Fig. 21 Local minimum structure of $Cs^+(H_2O)_{20}$ (non-dodecahedral) where the water molecules marked *black* indicate the pulled water molecules whereas the *white* water molecules indicate annealed rings which contain the pulled water molecule

Comparing the free energies obtained for the four different types of water molecules being pulled from the water network for $Cs^+(H_2O)_{19}$ and $Cs^+(H_2O)_{21}$ (see Table 2 for the actual values and Fig. 19 for a graphic representation of Table 2), one observes that for all temperatures the free energy of dissociation of the DA molecule of $Cs^+(H_2O)_{19}$ is lower than the free energy of dissociation of the other three. For $Cs^+(H_2O)_{21}$, however, the free energy of dissociation of the DA water molecule is lowest only for temperature $T \geq 80$ K. Comparing the values obtained for the two DA molecules with that obtained for the free energy of dissociation of one water molecule of the dodecahedron and the non-dodecahedron, the DA molecules beat all other values with respect to being the lowest in energy, with the exception of $Cs^+(H_2O)_{21}$ at $T = 40$ K. For temperatures of $T \leq 80$ K, the free energy of dissociation of DA molecules does not differ much from the values obtained for most of the three-coordinated molecules for $Cs^+(H_2O)_{20}$, $Cs^+(H_2O)_{21}$ and $Cs^+(H_2O)_{19}$. However when looking at $T \geq 120$ K, especially the free energy of dissociation of the DA molecule from $Cs^+(H_2O)_{21}$ is considerably lower compared to all others. The effect is also present for $Cs^+(H_2O)_{19}$, though not as pronounced. Hence one can assume that it is indeed easier for a DA molecule to be dissociated from the water network. Comparing the values of the free energy of dissociation of single water molecules of the dodecahedron with the non-dodecahedron, one observes for temperatures of $T \leq 80$ K that it is most of the time much harder to dissociate the water molecules from the non-dodecahedron especially for DDA molecules. This is yet another observation not in accord with the dodecahedron hypothesis.

When looking at the average force vs. distance graphs for $T = 120$ K (see Fig. 22), one also observes that for similar water molecules being pulled from the water network the curves of both structures are similar although the respective maxima and minima in the curves differ by their depths as was already found for the comparison of $Cs^+(H_2O)_{19}$ and $Cs^+(H_2O)_{21}$. Nevertheless, compared to average force vs. distance graphs of $Cs^+(H_2O)_{19}$ and $Cs^+(H_2O)_{21}$ the differences between the two sets of plots of $Cs^+(H_2O)_{20}$ are less pronounced.

In the case of the DAA molecules being pulled, the free energy of dissociation obtained for these water molecules is in all cases larger for the dodecahedron than for non-dodecahedron. However, the difference is not very significant, ranging between 0.2 and 5.5 kJ/mol at most. When looking at the two similar DDA molecules it is the other way round for $T = 120$ K, namely the free energies of dissociation of the water molecules pulled from the non-dodecahedron are higher by 4.2 and 0.6 kJ/mol, respectively. For $T = 150$ K the

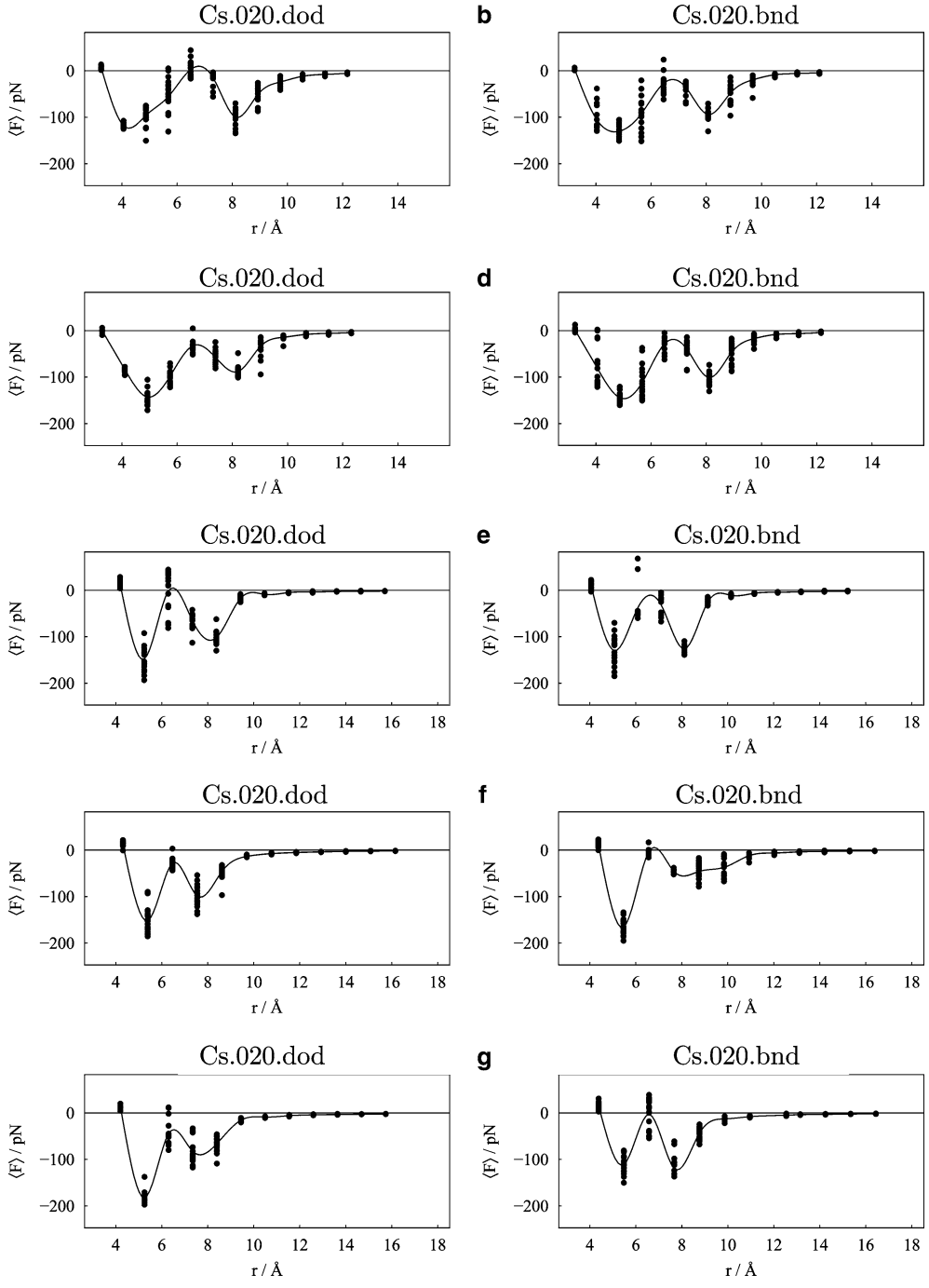

Fig. 22 Average constraint force $\langle F \rangle$ in pN vs. distance r in Ångström of pulled water molecules of structure Cs.020.dod.b for 18 starting conditions per distance r at $T = 120$ K

DDA of structure Cs.020.dod.d is better by 1.9 kJ/mol than that of the structure Cs.020.bnd.d, whereas for Cs.020.dod.b and Cs.020.bnd.b the non-dodecahedral structure beats the dodecahedral structure by 4.7 kJ/mol.

Hence neither the dodecahedron-shaped structure nor the non-dodecahedron-shaped structure was found to be better, as the differences between the two structures are too small to allow any conclusion and the differences would lead to conflicts anyway. Therefore it is impossible to ascribe the existence of the magic number $n = 20$ solely to the dodecahedron. However, it was found that it seems to be indeed easier to pull DA molecules from water networks compared to three-coordinated water molecules. As both the dodecahedron and the non-dodecahedron at $n = 20$ do not contain any of these DA water molecules in contrast to their immediate neighbours $n = 19$ and $n = 21$, this could lead to

Table 2 Free energy ΔG in kJ/mol for different water molecules being pulled from the cluster structures $Cs^+(H_2O)_{19}$, $Cs^+(H_2O)_{21}$ and $Cs^+(H_2O)_{20}$ (dodecahedral/dod and non-dodecahedral/bnd); for corresponding structures see Figs. 14, 15, 20 and 21; for a selection of average force vs distance graphs of $Cs^+(H_2O)_{19}$ and $Cs^+(H_2O)_{21}$ see Fig. 17 whereas for a complete set of all graphs of all systems see ref. [54].

Structure	Pulled H_2O	T (ΔGin KJ/mol)			
		40 K	80 K	120 K	150 K
Cs.019.a	DA	22.5	21.0	19.0	17.7
Cs.019.b	DDA	27.4	24.7	23.0	20.1
Cs.019.c	DAA	27.3	23.6	20.8	18.8
Cs.019.d	DDA	30.0	28.8	24.8	21.4
Cs.021.a	DA	28.9	19.8	15.1	14.2
Cs.021.b	DAA	27.5	25.6	22.2	19.7
Cs.021.c	DAA	25.2	25.0	22.9	21.4
Cs.021.d	DDA	30.6	28.5	26.4	24.5
Cs.020.dod.a	DDA	29.3	27.5	23.7	20.9
Cs.020.dod.b	DDA	29.4	27.2	23.9	19.7
Cs.020.dod.c	DDA	38.2	34.4	27.9	21.9
Cs.020.dod.d	DDA	35.6	32.0	28.3	25.3
Cs.020.dod.e	DAA	32.5	29.5	27.4	25.0
Cs.020.dod.f	DAA	27.6	25.4	23.4	20.9
Cs.020.dod.g	DAA	28.4	26.4	24.2	21.2
Cs.020.bnd.a	DDA	28.2	26.0	23.9	22.0
Cs.020.bnd.b	DDA	36.6	33.6	28.1	24.5
Cs.020.bnd.c	DDA	37.0	34.7	32.2	29.0
Cs.020.bnd.d	DDA	39.2	34.3	28.9	23.4
Cs.020.bnd.e	DAA	29.0	25.0	22.5	19.5
Cs.020.bnd.f	DAA	24.5	22.2	21.2	20.3
Cs.020.bnd.g	DAA	27.0	26.2	23.9	21.0

an explanation that $n = 20$ is magic due to cage inclusion compounds of various forms, exhibiting a water network of water molecules that are solely three- or four-coordinated. This nicely fits into the static picture already given in Sect. 3.1.1.

4 Conclusions

The purpose of this work was to obtain structural and dynamical information about alkali cation microhydration clusters, i.e. $Na^+(H_2O)_n$, $K^+(H_2O)_n$ and $Cs^+(H_2O)_n$ with $4 \leq n \leq 24$, both in general and with a special focus on cage inclusion compounds and magic numbers. The problem was approached using a combination of global geometry optimisation and molecular dynamics simulation.

As a first step, an extensive global geometry optimisation study has been carried out for these systems. The results obtained constitute a first unbiased and systematic overview on structures of alkali cation microhydration clusters and is also the first unbiased check of the dodecahedron hypothesis.[27, 54]. With a detailed analysis of pair interactions, reasons for structural trends could be provided. In a final step, molecular dynamics simulations were applied to all global minimum energy and selected low-lying local minimum energy cluster structures at different temperatures, simulating a canonical distribution. As reactions are a rare event to observe in cluster dynamics, constrained dynamics was used to force a dissociation reaction, to be able to compare the dissociation behaviour of different water cages and to allow the computation of free energies for the chosen dissociation reactions.

A molecular dynamics routine has been programmed from scratch for alkali cation microhydration clusters. As integration scheme, the velocity Verlet was chosen for the translational motion and a velocity Verlet-like rotational integrator for the rotational motion. The algorithm can generate microcanonical ensembles (default) and canonical ensembles via the Andersen thermostat. The algorithm also allows for a constraint, which forces a selected water molecule to stay at a fixed distance from the central ion.

All global minimum structures were submitted to molecular dynamics simulations using the canonical ensemble and a total simulation time of 10 ps with a time-step of 0.1 fs. It was found that for temperatures of $T \leq 80$ K mostly hindered rotational motion and very little hindered translational motion occurred for all three systems $Na^+(H_2O)_n$, $K^+(H_2O)_n$ and $Cs^+(H_2O)_n$. Upon increasing the temperature to $T = 150$ K, mostly the smaller cluster structures with $4 \leq n \leq 13$ exhibited strong structural changes. In larger clusters the water molecules start to form a cohesive network and the energy is distributed over more degrees of freedom. Hence, structural changes become less pronounced and also the effect of different starting conditions on structural variety decreases. For larger cluster sizes with $16 \leq n \leq 21$, mostly small rotational motion and to some extent very small translational motion can be observed as the water molecules are hindered by the network to move freely. This is in stark contrast to the frequent assumption that these systems are so flexible that the concept of "structure" itself loses its meaning. For $n = 20$ it was found that when using the canonical ensemble and comparing non-dodecahedron-shaped structures with dodecahedron structures for

all three systems, significant changes were observed only in the case of sodium: the dodecahedron cluster structure collapsed during the simulations towards a cluster structure very close to that of the global optimum (non-dodecahedral). Hence it could be shown that for sodium $n = 20$ is not a magic number due to a possible cage formation, as clearly non-dodecahedral and non-clathrate structures are strongly preferred energetically and easily accessible dynamically. In the case of potassium, no information could be gained by this comparison, whereas in the case of caesium at least at $T = 150$ K a small difference was observable, i.e. it was found that for the dodecahedron structure no bond openings were visible, whereas they sometimes occurred for non-dodecahedron structures and then mostly between annealed four- and six-membered rings. Hence this is a weak support of the dodecahedron hypothesis in case of $Cs^+(H_2O)_{20}$.

In the special case of $Cs^+(H_2O)_{20}$, and for the neighbouring $Cs^+(H_2O)_{19}$ and $Cs^+(H_2O)_{21}$, constrained dynamics simulations were run, enforcing dissociation of single water molecules. This allowed for the computation of the free energy of dissociation of these water molecules. The single water molecules to be pulled from the water network have been selected such that they were comparable to each other with respect to similar surroundings or equivalent coordination patterns. For the two structures $Cs^+(H_2O)_{20}$, i.e. the dodecahedron and the non-dodecahedron, no significant differences could be observed for the free energies of dissociating single water molecules. In other words neither of the structures was less stable than the other. Hence no further proof could be gained that the magic number $n = 20$ is solely due to the formation of a dodecahedron-shaped water network. However, when comparing the immediate neighbours of $Cs^+(H_2O)_{20}$, i.e. $Cs^+(H_2O)_{19}$ and $Cs^+(H_2O)_{21}$, to $Cs^+(H_2O)_{20}$ it was found that it was indeed easier to pull off the DA (single donor–single acceptor) molecules and for that matter also their two adjacent molecules, respectively, from the water networks. As both structures investigated for $n = 20$ do not contain any DA molecule, this is some support for the magic number 20 being due to cage structures in general, containing solely three- or four-coordinated water molecules. Therefore, we propose to replace the dodecahedron hypothesis by a simpler but possibly more robust hypothesis, namely that the magic number $n = 20$ (but also others) observed in $K^+(H_2O)_n$ and $Cs^+(H_2O)_n$ are due to several different lowest-energy cage structures that do not contain any weakly bound DA molecules that are susceptible to dissociation and association reactions. Due to the smallness and the stronger "structure breaking" effect of $Na^+(H_2O)_n$, these cage structures collapse quickly to very different off-centred structures in the case of $Na^+(H_2O)_n$. These three-dimensional networks follow totally different build-up principles and hence do not show the magic number pattern of the cage structures.

There are many ways to extend these investigations. At first one might stay within the given model potential and compute MD simulations using other local minimum energy structures as input geometries to better compare different structures of one cluster size. Also a larger variety of different starting conditions should be tested. To further clarify the structural pattern found for magic number cluster structures it is also possible to force other dissociation reactions than that investigated in this work or for that matter also association reactions. As the TIP4P/OPLS potential is not always reliable in producing correct energy differences between different isomers, it would also be necessary to employ better model potentials which allow for flexible water molecules, polarisation and possibly even OH-bond rupture. Another possibility would be to use ab initio potentials for the simulations; however, this is still too expensive to realise on a sufficiently large scale. Currently, we are improving the relative energy ordering of our best structures by local re-optimisation at suitable ab initio levels. We are also simulating IR-spectra in the OH-stretch region and directly comparing them to experimental spectra [54, F. Schulz et al., in preparation]. This will allow us to test our predictions of magic number structures directly in the near future.

Acknowledgements It is a pleasure for B.H. to thank Prof. Dr. Hermann Stoll for his kind and competent help and cooperation in research and teaching during many years in neighbouring offices at the University of Stuttgart. In connection with the present work, we would like to thank James M. Lisy for helpful discussions. We thank the DFG for the financial support of this project. Thanks also go to the computer centre in Kiel for computer time and technical support.

References

1. Liu K, Cruzan JD, Saykally RJ (1996) Science, 271: 929
2. Castleman AW Jr, Bowen KH (1996) J Phys Chem 100: 12911
3. Niedner-Schatteburg G, Bondybey VE (2000) Chem Rev 100: 4059
4. Duncan MA (1997) Annu Rev Phys Chem 48: 69
5. Lisy JM (1997) Int Rev Phys Chem 16: 267
6. Buck U, Huisken F (2000) Chem Rev 100: 3863
7. Sobott F, Wattenberg A, Barth H-D, Brutschy B (1999) Int J Mass Spectr 185–187: 271
8. Lee S-W, Freivogel P, Schindler T, Beauchamp JL (1998) J Am Chem Soc 120: 11758
9. Kim J, Lee S, Cho SJ, Mhin BJ, Kim KS (1995) J Chem Phys 102: 839
10. Lee HM, Kim J, Lee S, Mhin BJ, Kim KS (1999) J Chem Phys 111: 3995
11. Lybrand TP, Kollman PA (1985) J Chem Phys 83: 2923
12. Cieplak P, Lybrand TP, Kollman PA (1987) J Chem Phys 86: 6393
13. Sung S-S, Jordan PC (1986) J Chem Phys 85: 4045
14. Lin S, Jordan PC (1988) J Chem Phys 89: 7492
15. Balbuena PB, Wang L, Li T, Derosa PA (1999) In: Balbuena PB, Seminario JM (eds) Molecular dynamics. From classical to quantum methods. Theoretical and computational chemistry, Vol 7. Elsevier, Amsterdam, p 431
16. Holland PM, Castleman AW, Jr (1980) J Chem Phys 72: 5984
17. Kassner JL Jr, Hagen DE (1976) J Chem Phys 64: 1860
18. Jeffrey GA (1984) In: Atwood JL, Davies JED, MacNiol DD (eds) Inclusion compounds, vol 1. Academic Press, New York, Chap. 5
19. Lipkowski J (1996) In: Webbs GA (ed.) Annual reports on the progress of chemistry, section C, vol 96. The Royal Society of Chemistry, Cambridge, Chap. 10
20. Koh CA, Wisbey RP, Wu X, Westacott RE, Soper AK (2000) J Chem Phys 113: 6390
21. Førrisdahl OK, Kvamme B, Haymet (1996) ADJ Mol Phys 89: 819
22. Khan A (1994) Chem Phys Lett 217: 443

23. Wei S, Shi Z, Castleman AW, Jr. (1991) J Chem Phys 94: 3268
24. Hulthe G, Stenhagen G, Wennerström O, Ottosson C-H (1997) J Chromat A 777: 155
25. Blokzijl W, Engberts JBFN (1993) Angew Chem 105: 1610
26. Head-Gordon T (1995) Proc Natl Acad Sci USA 92: 8308
27. Schulz F, Hartke B (2002) Chem Phys Chem 3: 98
28. Tongraar A, Liedl KR, Rode BM (1998) J Phys Chem. A 102: 10340
29. Horst R, Pardalos PM, Thoai NV (2000) In: Nonconvex optimization and its applications. Kluwer, Dordrecht
30. Wille LT (2000) In Stauffer D (ed) Annual reviews of computational physics VII. World Scientific, Singapore
31. Hartke B (1993) J Phys Chem 97: 9973
32. Gregurick SK, Alexander MH, Hartke B (1996) J Chem Phys 104: 2684
33. Hartke B (1999) J Comput Chem 20: 1752
34. Hartke B (2000) Z Phys Chem 214: 1251
35. Hartke B, Schütz M , Werner H-J (1998) Chem Phys 239: 561
36. Hartke B, Charvat A, Reich M, Abel B (2002) J Chem Phys 216: 3588
37. Hodges MP (2004) Program xmakemol, http://www.nongnu.org/xmakemol/, version 5.15
38. Hartke B (1996) Chem Phys Lett 258: 144
39. Jorgensen WL (1982) J Chem Phys 77: 4156
40. Chandrasekhar J, Spellmeyer DC, Jorgensen WL (1984) J Am Chem Soc 106: 903
41. Lee SH, Rasaiah JC (1994) J Chem Phys 101: 6964
42. Reddy MR, Berkowitz M (1988) J Chem Phys 88: 7104
43. Hartke B (2002) Angew Chem 114: 1534
44. Hartke B 2001 In: Spector L, Goodman E, Wu A, Langdon WB, Voigt H-M, Gen M, Sen S, Dorigo M, Pezeshk S, Garzon M , Burke E (eds) Proceedings of the genetic and evolutionary computation conference, GECCO-2001. Morgan Kaufmann, San Francisco, p 1284
45. Hartke B (1998) Theor Chem Acc 99: 241
46. Frenkel D, Smit B (2002) Understanding molecular simulation. Academic, New York
47. Gaberoglio G (2001) Dynamical properties of H-bonded liquids: a theoretical and computer simulation study, PhD Thesis: Università Degli Studi di Trento, Italy
48. Mülders T, Krüger P, Swegat W, Schlitter JJ (1996) Chem Phys 104: 4869
49. Schlitter J, Swegat W, Mülders T (2001) J Mol Mod 7: 171
50. Swegat W, Schlitter J, Krüger P, Wollmer A (2003) Bio Phys J 84: 1493
51. Andersen HC (1983) J Comput Phys 52: 24
52. Schulz F (2001) Diploma thesis. University of Stuttgart, Germany
53. Wales DJ (2003) Energy landscapes: with applications to clusters, biomolecules and glasses. Cambridge Molecular Science, Cambridge
54. Schulz F (2005) Structure, spectra, and dynamics of alkali cation microhydration clusters, PhD Thesis. University Kiel, Germany
55. Nauta K, Miller RE (2000) Science 287: 293
56. Wales DJ, Hodges MP (1998) Chem Phys Lett 286: 65
57. Liu K, Brown MG, Saykally RJ (1996) J Phys Chem. A 101: 501
58. Sadlej J, Buch V, Kazimirski JK, Buck U (1999) J Phys Chem. A 103: 4933
59. Klopper W, Luethi HP (1999) Mol Phys 96: 559
60. Jortner J (1992) Z Phys D – Atoms, Molecules Clusters 24: 247
61. Selinger A, Castleman AW, Jr. (1991) J Phys Chem 95: 8442
62. Rick SW, Stuart SJ, Berne BJ (1994) J Chem Phys 101: 6141
63. Burnham CJ, Li J, Xantheas SS, Leslie M (1999) J Chem Phys 110: 4566